Electronic Research Archive

https://www.aimspress.com/journal/era

ERA, 32(10): 5682–5716.
DOI: 10.3934/era.2024263
Received: 02 September 2024
Revised: 09 October 2024
Accepted: 12 October 2024
Published: 16 October 2024

Research article

Dynamics analysis of a predator-prey model with Allee effect and harvesting effort

Yichao Shao[1], Hengguo Yu[1,2,*], Chenglei Jin[1], Jingzhe Fang[1] and Min Zhao[2*]

[1] School of Mathematics and Physics, Wenzhou University, Wenzhou 325035, China

[2] Key Laboratory for Subtropical Oceans & Lakes Environment and Biological Resources Utilization Technology of Zhejiang, Wenzhou University, Wenzhou 325035, China

* **Correspondence:** Email: yuhengguo5340@163.com, zhaomin-zmcn@tom.com.

Abstract: In the paper, a predator-prey model with the Allee effect and harvesting effort was proposed to explore the interaction mechanism between prey and predator. Under the framework of mathematical theory deduction, some conditions for the occurrence of transcritical, saddle-node, Hopf, and Bogdanov-Takens bifurcations were derived with harvesting effort and the Allee effect as key parameters. Under the framework of bifurcation dynamics numerical simulation, the evolution process of specific bifurcation dynamics behavior was gradually visualized to reveal the influence mechanism of the Allee effect and harvesting effort. The research results indicated that the Allee effect and harvesting effort not only seriously affected the bifurcation dynamics essential characteristics of the model (1.3), but also could promote the formation of constant steady state and periodic oscillation persistent survival mode of prey and predator. Furthermore, it is worth noting that appropriate harvesting effort was beneficial for the formation of a sustainable survival cycle between prey and predator. In summary, we hoped that the research findings could contribute to the comprehensive promotion of bifurcation dynamics studies in the predator-prey model.

Keywords: predator-prey system; Allee effet; harvesting effort; persistent survival mode; evolutionary trend

1. Introduction

As has well known, with the rapid development of the global economy and society, water eutrophication has become a global water environmental problem [1, 2]. Furthermore, in order to economically and efficiently assess and respond to natural environmental challenges, theoretical ecologists and mathematicians have delved into complex ecosystems by developing some ecological mathematical models, so that the interactions between prey and predator have consistently been a focal point of ecological

research [3].

In the 1920s, Lotka [4] and Volterra [5] introduced the first predator-prey model. Since then, scholars have investigated the interactions between predator and prey influenced by various ecological factors, such as environmental pollution, fishing practice, prey refuge, fear, supplementary food sources, and diseases [6–13], and obtained some excellent research results. The paper [6] examined dynamical behaviors of a predator-prey system with foraging facilitation and group defense, and found that both foraging facilitation and group defense mechanisms could play an important role in promoting the balance and diversity of researchers. The researchers [7] proposed a two-species model of mammalian prey and mammalian predator, and found that water resources could play a crucial role in shaping the dynamics between mammalian prey and mammalian predator. Researchers [8] revealed the fact that some species in the ecosystem suddenly burst back many years after almost being extinct. The researchers in [9] considered a predator-prey model with fear-induced group defense and Monod-Haldane functional response, and highlighted the complex interplay of fear effect, group defense, and anti-predator sensitivity in predator-prey dynamics. The researchers in [10] raised a mathematical model with Holling type II functional response and nonlinear harvesting, and elucidated the dual impact of harvesting and the presence of invasive species. The researchers in [11] discussed the dynamics and optimal harvesting of a prey-predator fishery model by incorporating the nonlinear Michaelis-Menten type of harvesting in predator, and derived the optimal threshold for the predator harvesting, which could give maximum financial profit to sustain the fishery resources. The researchers in [12] explored two kinds of reaction-diffusion predator-prey systems with quadratic intra-predator interaction and linear prey harvesting, and disclosed that the intra-predator interaction and prey harvesting could have a significant effect on the spatiotemporal pattern formations. The researchers in [13] constructed a cross-diffusive predator-prey model with the inclusion of prey refuge, and revealed that the interaction of both self- and cross-diffusion could play a significant role on the pattern formation.

However, departing from the Lotka-Volterra predator-prey model, forward-thinking mathematicians refined a predator-prey model, which can result in the enhanced Leslie-Gower ameliorated predator-prey model [14, 15]. The Leslie-Gower ameliorated predator-prey model typically takes the following form [16]:

$$\begin{cases} \dot{x} = r_1 x(1 - \frac{x}{K}) - f(x)y, \\ \dot{y} = r_2 y(1 - \frac{y}{hx}), \end{cases} \tag{1.1}$$

where $f(x)$ is named a Leslie–Gower term. Clearly, various functional response functions $f(x)$ and ecological factors exert distinct impacts, which can lead to diverse outcomes. Consequently, numerous scholars have explored different functional response functions and ecological factors through the Leslie-Gower predator-prey model, such as these papers [17–26]. The researchers in [17] considered a predator-prey model with fear effect and inquired into the occurrence of Turing, Hopf and Turing-Hopf bifurcation. The researchers in [18] formulated a three-species food chain model to investigate the impact of fear and discovered that the fear effect could transform the system from chaotic dynamics to a stable state. The researchers in [19] constructed a slow-fast predator-prey system with group defense of the prey and revealed that some certain species in the ecosystem suddenly burst back many years after being about extinct. The researchers in [20] discussed a predator-prey model with prey refuge and explored the local bifurcation and stability of the limit cycle. The researchers in [21] described a prey-predator system with constant prey refuge and their objective was to maximize the monetary social benefit through protecting the predator species from extinction. The researchers in [22] examined

the influence of the Allee effect in a prey-predator interaction model with a generalist predator, and found that Allee effect could turn the system more structurally stable compared to prey-predator model with generalist predator. The researchers in [23] investigated the local and global dynamics of the prey-predator model with emphasis on the impact of strong Allee effect. The researchers in [24] investigated dynamics of non-autonomous and autonomous systems based on the Leslie–Gower predator-prey model using the Beddington-DeAngelis functional response. The researchers in [25] proposed a three-species food chain model to survey the impact of fear and found that fear effect could transform the system from chaotic dynamics to a stable state. The researchers in [26] constructed an aquatic ecological model to describe the aggregation effect of Microcystis aeruginosa.

Furthermore, in 1931, the researchers in [27] observed the fluctuations in complex populations and concluded that when population density fell below a certain threshold, the birth rate decreased while the mortality rate increased, which was known as the Allee effect. Some researchers [28–32] incorporated the Allee effect into the predator-prey model, explored the impact of Allee effect on the interaction between predator and prey, and achieved some excellent research results. The researchers in [28] considered a Leslie-Gower predator-prey model with the Allee effect in prey and illustrated the impact in the stability of positive equilibrium point by adding an Allee effect. The researchers in [29] proposed a Leslie-Gower predator-prey model with the Allee effect and revealed the influence of Allee effect on the dynamic behaviors. The researchers in [30] established a phytoplankton-zooplankton model with a strong Allee effect, and pointed out that the Allee threshold for the phytoplankton population could significantly influence the overall dynamics. The researchers in [31] dealt with an eco-epidemiological predator-prey model with the Allee effect and noted Allee effect had an important and fundamental aspect on population growth. The researchers in [32] investigated dynamical behavior of a discrete logistic equation with the Allee effect, theoretically and numerically investigated some bifurcation dynamical behaviors, and provided some important dynamic results.

The Beddington-DeAngelis functional response was randomly disturbed by the well-known mean-reverting Ornstein-Uhlenbeck process [33], and the main difference of this functional response from other functional responses was that it contained an extra term presenting mutual interference by predators, meaning that the predator population density seriously affected the predation dynamic mechanism. Thus, the Beddington-DeAngelis functional response could significantly affect the stability of the Leslie-Gower predator-prey model. Some researchers [34–36] introduced Beddington-DeAngelis functional response into the predator-prey model, explored its impact on dynamic behavior, and yielded some significant results. The researchers in [34] investigated the complex dynamics in a discrete-time predator-prey model with a Beddington–DeAngelis functional response, and determined that the model could exhibit rich complexity features such as stable, periodic, and chaotic dynamics. The researchers in [35] discussed the dynamic complexities of a three-species food chain with Beddington-DeAngelis functional response and concluded that the model had dynamic properties. The researchers in [36] developed a predator-prey model with a Beddington-DeAngelis functional response and indicated that the model could appear in a series of complex phenomenon, such as period-doubling, chaos attractor, and period-halfing. Based on the above research results, it can be concluded that Beddington-DeAngelis functional response can cause the predator-prey model to have more diverse dynamic behaviors; we apply the Beddington-DeAngelis functional response to describe the dynamic relationship between predator and prey with sufficient accuracy in this paper.

The focus on sustained harvesting effort was crucial in the study of the predator-prey model [37].

Some researchers in [38–40] investigated how harvesting factors influence the dynamic relationship between predator and prey, and achieved some important results. The researchers in [38] explored a predator-prey model to evaluate the impacts of harvesting and summarized that the harvesting of predators was beneficial and could promote the coexistence of species only when their growth from other food sources was too much. The researchers in [39] proposed a predator-prey model with constant-yield prey harvesting and confirmed that the constant-yield prey harvesting could drive both species to extinction suddenly. The researchers in [40] constructed a predator-prey system with harvesting, and pointed out that harvesting efforts could generate a region of stability.

Moreover, specific dynamic behavior has always been one of the hot research topics in many fields, and some good results have been obtained in these papers [41–48]. The researchers in [41] found that the nonlocal fear effect could enable the system to exhibit Hopf bifurcation and Turing-Hopf bifurcation. The researchers in [42] provided some discussion of the persistence and extinction of the infective population and examined the global asymptotic stability of the equilibrium point. The researchers in [43] indicated that Turing instability could be induced by the negative diffusion coefficients. The researchers in [44] studied stability and local bifurcation of semi-trivial steady-state solutions. The researchers in [45] investigated global stability of the disease-free equilibrium point in a diffusion system. The researchers in [46] analyzed the existence of Hopf bifurcation by analyzing the distribution of the characteristic values. The researchers in [47] inquired into some threshold dynamical behaviors for extinction or continuous persistence of disease. The researchers in [48] discussed global stability of unique endemic equilibrium point by constructing suitable Lyapunov function.

In this paper, we explore a predator-prey model with a Beddington-DeAngelis functional response functions, the Allee effect, and harvesting effort, namely:

$$\begin{cases} \dot{\overline{x}} = r\overline{x}(1-\frac{\overline{x}}{K})(\overline{x}-M) - \frac{\alpha\overline{x}\overline{y}}{1+\overline{b}\overline{x}+\overline{c}\overline{y}} - q_1 m_1 e_1 \overline{x}, \\ \dot{\overline{y}} = s\overline{y}(1-\frac{\overline{y}}{h\overline{x}}) - q_2 m_2 e_2 \overline{y}. \end{cases} \tag{1.2}$$

where $\overline{x}(\bar{t})$ and $\overline{y}(\bar{t})$ represent the population densities of prey and predator respectively, r and s represent the intrinsic growth rate of prey and predator respectively, K is maximum environmental capacity, M represents the Allee effect threshold ($0 < M < K$), α stands for maximum predation rate, $\overline{b}$ and $\overline{c}$ are the half-saturation constant and the functional response constant respectively, q_1 is the catchability co-efficient of prey, m_1 represents the part of prey that can be harvested, e_1 is the effort value for the harvest from prey, h is used to measure the food quality of prey in order to transform them into offspring of predator, q_2 is the catchability co-efficient of predator, m_2 represents the part of predator that can be harvested, e_2 is the effort value for the harvest from predator. Moreover, it is worthy of our recognition that the main advantage of the model (1.2) is the introduction of the Allee effect and harvesting effort, which not only creates a critical threshold for the extinction and persistence of prey population, but also regulates the persistent survival mode between prey and predator. Furthermore, it is obvious to know that the unit growth function of the prey population is $f(\overline{x})) = r(1-\frac{\overline{x}}{K})(\overline{x}-M)$, then we have $\frac{df(\overline{x})}{d\overline{x}} = \frac{r(M+K)-2r\overline{x}}{K}$. Thus, we can obtain $\frac{df(\overline{x})}{d\overline{x}}|_{\overline{x}=0} = \frac{r(M+K)}{K} > 0$, $f(0) = -rM < 0$ and $f(\frac{M+K}{2}) = \frac{r(K-M)^2}{4K} > 0$. According to the conditions satisfied by the strong Allee effect, it can be inferred that the Allee effect introduced in this model is a strong Allee effect.

By performing some straightforward conversions and simplifications, the following transformations

were given:

$$x = \frac{\overline{x}}{K}, \quad t = r\bar{t}K, \quad y = \frac{\alpha\overline{y}}{rK}, \quad m = \frac{M}{K}.$$

Then we transform the model (1.2) into (1.3)

$$\begin{cases} \dot{x} = x(1-x)(x-m) - \frac{xy}{1+bx+cy} - \lambda_1 x, \\ \dot{y} = \delta y(\beta - \frac{y}{x}) - \lambda_2 y, \end{cases} \tag{1.3}$$

where $b = \overline{b}K, c = \frac{\overline{c}rK}{\alpha}, \delta = \frac{s}{\alpha Kh}, \beta = \frac{\alpha h}{r}, \lambda_1 = \frac{q_1 m_1 e_1}{rK}, \lambda_2 = \frac{q_2 m_2 e_2}{rK}$ are positive constants.

The framework of the paper is organized as follows: In Section 1, we introduce the origin and theoretical basis. In Section 2, the boundedness of the model (1.3) is analyzed. In Sections 3 and 4, the existence and stability of the equilibrium points of the model (1.3) are discussed. In Section 5, the transcritical bifurcation, saddle-node bifurcation, Hopf bifurcation, and Bogdanov-Takens bifurcation in the model (1.3) are studied. In Section 6, numerical simulation experiments are conducted to explore the dynamic behaviors and expound the biological significance. In Section 7, based on the analysis and research of the previous six sections, a brief conclusion is given.

2. Boundedness of the solutions

In this section, we first examine the limits of $x(t)$ and $y(t)$ in the model (1.3) to facilitate a subsequent dynamic analysis.

Theorem 2.1. *Under the initial conditions, the solution for the model (1.3) remains positive at all times:* $(x(0), y(0)) \in \Omega = \left\{(x, y) \in R^2 \mid x > 0, y > 0\right\}$.

Proof. Based on the model's conditions, we can perceive the boundary using the equation below:

$$x(t) = x(0)exp\left\{\int_0^t (1 - x(\zeta))(x(\zeta) - m) - \frac{y(\zeta)}{1 + bx(\zeta) + cy(\zeta)} - \lambda_1 d\zeta\right\},$$
$$y(t) = y(0)exp\left\{\int_0^t \delta(\beta - \frac{y(\zeta)}{x(\zeta)}) - \lambda_2 d\zeta\right\}.$$

Therefore, the model (1.3) typically exhibits its most common boundary $\left\{(x, y) \in R^2 \mid x > 0, y > 0\right\}$. Next, we investigate the bounds of $x(t)$ and $y(t)$ through the two equations associated with the model (1.3), respectively. □

Theorem 2.2. *As long as the model (1.3) satisfies* $\lambda_2 < \delta\beta$, *the range of* $x(t)$ *and* $y(t)$ *in the model (1.3) can be confined to a positive set:*

$$\Omega = \left\{(x(t), y(t)) \in R_+^2 \mid 0 < x(t) < 1, 0 < y(t) < \beta - \frac{\lambda_2}{\delta}\right\}.$$

Proof. We pay attention to the first equation of the model (1.3), and give the following scaling form:

$$\dot{x} < x(1 - x)(x - m).$$

Regarding this equation, we will analyze and discuss three scenarios to determine the approximate range of $x(t)$:

1) If $x(t) > 1$, then $\dot{x} < 0$.

2) If $0 < x(t) < m$, then $\dot{x} < 0$.

3) If $m < x(t) < 1$, then $x(t) < 1 - \frac{1}{1+C_1e^{(1-m)t}}$, so $\lim\limits_{t\to+\infty} supx(t) \leq 1$.

The first and second points are self-evident, let us scale it up and down

$$\dot{x} < x(1-x)(1-m),$$

then

$$(\frac{1}{x} + \frac{1}{1-x})dx < (1-m)dt.$$

Simplify through integration on both sides, we can get

$$\frac{x}{1-x} < C_1e^{(1-m)t},$$

then

$$x < 1 - \frac{1}{1+C_1e^{(1-m)t}}.$$

Obviously, if $x(t) > 1$, then $\dot{x} < 0$. If $0 < x(t) < m$, then $\dot{x} > 0$. If $m < x(t) < 1$, then $x(t) < 1 - \frac{1}{1+C_1e^{(1-m)t}}$, so $0 < x(t) < 1$ when $(x(t), y(t)) \in R^2_+$. Then we pay attention to the second equation of the model (1.3), give the following scaling form:

$$\dot{y} < \delta y(-y + \beta - \frac{\lambda_2}{\delta}).$$

Regarding this equation, we will analyze and discuss two scenarios to determine the approximate range of $y(t)$:

1) If $y \geq \beta - \frac{\lambda_2}{\delta}$, then $\dot{y} < 0$. This contradicts the positive solution of $y(t)$ in Theorem 2.1.

2) If $0 < y < \beta - \frac{\lambda_2}{\delta}$, then $y(t) < \beta - \frac{\lambda_2}{\delta} - \frac{\beta - \frac{\lambda_2}{\delta}}{1+C_2e^{\delta(\beta-\frac{\lambda_2}{\delta})t}}$, so $\lim\limits_{t\to+\infty} supy(t) \leq \beta - \frac{\lambda_2}{\delta}$.

The first point is self-evident, so let's focus on proving the second one:

$$(\frac{1}{y} + \frac{1}{\beta - \frac{\lambda_2}{\delta} - y})dy < \delta(\beta - \frac{\lambda_2}{\delta})dt.$$

Simplify through integration on both sides, we can get

$$\frac{y}{\beta - \frac{\lambda_2}{\delta} - y} < C_2e^{\delta(\beta-\frac{\lambda_2}{\delta})t},$$

then, we can obtain

$$y < \beta - \frac{\lambda_2}{\delta} - \frac{\beta - \frac{\lambda_2}{\delta}}{1 + C_2e^{\delta(\beta-\frac{\lambda_2}{\delta})t}}.$$

By calculation, we can clearly see $\lim\limits_{t\to+\infty} supy(t) \leq \beta - \frac{\lambda_2}{\delta}$. Based on the prior discussions regarding $x(t)$ and $y(t)$, we can infer that the model (1.3) is subject to specific boundaries, and we encapsulate this conclusion within a set:

$$\Omega = \left\{(x(t), y(t)) \in R^2_+ \mid 0 < x(t) < 1, 0 < y(t) < \beta - \frac{\lambda_2}{\delta}\right\}.$$

□

3. The existence of all possible equilibrium points

The existence of all possible equilibrium points in the model (1.3) is particularly important, which is the foundation for bifurcation dynamical research and indicates that prey and predator can remain stable in a certain state. In this section, the existence of all possible equilibrium points in the model (1.3) is carefully studied.

Based on the prey population equation $F(x)$ and the predator population equation $G(x)$, we convert the model (1.3) into the equation system (3.1) in order to more effectively expose the dynamical behavior at the equilibrium point, the equation as following:

$$\begin{cases} F(x) = x(1-x)(x-m) - \frac{xy}{1+bx+cy} - \lambda_1 x = 0, \\ G(x) = \delta y(\beta - \frac{y}{x}) - \lambda_2 y = 0. \end{cases} \tag{3.1}$$

If $(m+1)^2 - 4(m+\lambda_1) > 0$ holds, then we can obtain that the model (1.3) has two boundary equilibrium points, a predator-free equilibrium point $E_1(x_1, 0)$ and a predator-free equilibrium point $E_2(x_2, 0)$, where x_1 and x_2 are the roots of the equation:

$$x^2 - (m+1)x + m + \lambda_1 = 0,$$

solving the above equation, we can obtain x_1 and x_2 as

$$x_1 = \frac{m+1-\sqrt{(m+1)^2 - 4(m+\lambda_1)}}{2},$$
$$x_2 = \frac{m+1+\sqrt{(m+1)^2 - 4(m+\lambda_1)}}{2}.$$

It is obvious to find that there is only one boundary equilibrium point $(\frac{m+1}{2}, 0)$ when $(m+1)^2 - 4(m+\lambda_1) = 0$ holds. However, at this juncture, the absence of an internal equilibrium point in the model (1.3) renders it unsuitable for our intended study on internal equilibrium points. Consequently, to ensure the existence of such a point, we must fulfill certain prerequisites which need to satisfy $(m+1)^2 - 4(m+\lambda_1) > 0$, where x^* and y^* are the roots of the equation:

$$\begin{cases} x^*(1-x^*)(x^*-m) - \frac{x^*y^*}{1+bx^*+cy^*} - \lambda_1 x^* = 0, \\ \delta y^*(\beta - \frac{y^*}{x^*}) - \lambda_2 y^* = 0. \end{cases} \tag{3.2}$$

From the second equation of the equation system (3.2), we can get $y = (\beta - \frac{\lambda_2}{\delta})x$. From section two, we can get $\beta - \frac{\lambda_2}{\delta} > 0$. Integrate the first equation with the second equation, we can get the Eq (3.3):

$$\varphi x^3 + [1-(m+1)\varphi]x^2 + [(m+\lambda_1)\varphi + \gamma - (m+1)]x + (m+\lambda_1) = 0. \tag{3.3}$$

Let

$$\gamma = \beta - \frac{\lambda_2}{\delta}, \quad \varphi = b + c\gamma,$$

$$f(x) = \varphi x^3 + [1 - (m+1)\varphi]x^2 + [(m+\lambda_1)\varphi + \gamma - (m+1)]x + (m+\lambda_1),$$

$$g(x) = 3\varphi x^2 + 2[1 - (m+1)\varphi]x + (m+\lambda_1)\varphi + \gamma - (m+1),$$

$$A = [1 - (m+1)\varphi]^2 - 3\varphi[(m+\lambda_1)\varphi + \gamma - (m+1)],$$

$$B = [1 - (m+1)\varphi][(m+\lambda_1)\varphi + \gamma - (m+1)] - 9\varphi(m+\lambda_1),$$

$$C = [(m+\lambda_1)\varphi + \gamma - (m+1)]^2 - 3[1 - (m+1)\varphi](m+\lambda_1),$$

$$\Delta = B^2 - 4AC.$$

Theorem 3.1. *For the number of positive internal equilibrium points, we have:*

(1) If $A = B = 0$ holds, then the model (1.3) does not have any internal positive equilibrium point.

(2) If $\Delta > 0$ holds, then the model (1.3) does not have any positive equilibrium point.

(3) If $\Delta = 0$ holds, then the model (1.3) has a positive equilibrium point E_1^* or E_2^*, where x_1^*, x_2^* are dual positive roots.

(4) If $\Delta < 0$ holds, then the model (1.3) has two single positive equilibrium points E_3^* and E_4^* or E_5^* and E_6^*.

Proof. For the number of positive internal equilibrium points, we have:

1) When $A = B = 0$ holds, according to Cardano formula, then Eq (3.3) has a triple real root, and according to Descartes sign rule, when $1 - (m+1)\varphi \leqslant 0$ and $(m+\lambda_1)\varphi + \gamma - (m+1) \leqslant 0$ hold, obtaining a triple negative root is not helpful for our model research, so it is omitted.

2) When $\Delta > 0$ holds, according to Cardano formula, then Eq (3.3) has a real root and a pair of conjugate imaginary roots.

(i) When $1 - (m+1)\varphi > 0$ and $(m+\lambda_1)\varphi + \gamma - (m+1) > 0$ hold, according to Descartes sign rule, then Eq (3.3) has a negative root and not have positive root.

(ii) When $1 - (m+1)\varphi < 0$ and $(m+\lambda_1)\varphi + \gamma - (m+1) > 0$ hold, according to Descartes sign rule, then Eq (3.3) does not have a positive root or has two negative roots, thus the model (1.3) does not have positive root.

(iii) When $1 - (m+1)\varphi > 0$ and $(m+\lambda_1)\varphi + \gamma - (m+1) < 0$ hold, for the same reason (ii), Eq (3.3) does not have positive internal equilibrium point.

(iv) When $1 - (m+1)\varphi < 0$ and $(m+\lambda_1)\varphi + \gamma - (m+1) < 0$ hold, for the same reason (i), Eq (3.3) does not have positive root. Thus, when $\Delta > 0$ holds, Eq (3.3) does not have positive root, that is to say, the model (1.3) does not have any internal positive equilibrium point.

3) When $\Delta = 0$ holds, according to Cardano formula, then Eq (3.3) has three real roots, including one double root.

(i) When $1 - (m+1)\varphi > 0$ and $(m+\lambda_1)\varphi + \gamma - (m+1) > 0$ hold, according to Descartes sign rule, then the equation (3.3) has three negative roots, including one double negative root.

(ii) When $1 - (m+1)\varphi < 0$ and $(m+\lambda_1)\varphi + \gamma - (m+1) > 0$ hold, according to Descartes sign rule and Vieta theorem for univariate cubic equations, $x_1 + x_2 + x_3 < 0$ and $x_1x_2x_3 < 0$, thus Eq (3.3) has a double negative root and a single negative root.

(iii) When $1 - (m+1)\varphi > 0$ and $(m+\lambda_1)\varphi + \gamma - (m+1) < 0$ hold, according to Descartes sign rule and Vieta theorem for univariate cubic equations, $x_1 + x_2 + x_3 > 0$, $x_1x_2x_3 < 0$, thus Eq (3.3) has a double positive root and a negative root, then the model (1.3) has a positive equilibrium point $E_1^* = (x_1^*, y_1^*)$, where x_1^* is a dual positive root.

(iv) When $1-(m+1)\varphi < 0$ and $(m+\lambda_1)\varphi+\gamma-(m+1) < 0$ hold, according to Descartes sign rule and Vieta theorem for univariate cubic equations, $x_1+x_2+x_3 > 0, x_1x_2x_3 < 0$, thus Eq (3.3) has a double positive root and a negative root, then the model (1.3) has a positive equilibria point $E_2^* = (x_2^*, y_2^*)$, where x_2^* is a dual positive root. Thus, when $\Delta = 0$, the model (1.3) has a positive equilibrium points E_1^* or E_2^* under certain conditions.

4) When $\Delta < 0$ holds, according to Cardano formula, then Eq (3.3) has two unequal real roots.

(i) When $1-(m+1)\varphi > 0$ and $(m+\lambda_1)\varphi+\gamma-(m+1) > 0$ hold, according to Descartes sign rule and Vieta theorem for univariate cubic equations, $x_1+x_2+x_3 < 0, x_1x_2x_3 < 0$, thus Eq (3.3) has three single negative roots.

(ii) When $1-(m+1)\varphi < 0$ and $(m+\lambda_1)\varphi+\gamma-(m+1) > 0$ hold, for the same reason (i), Eq (3.3) does not have positive root.

(iii) When $1-(m+1)\varphi > 0$ and $(m+\lambda_1)\varphi+\gamma-(m+1) < 0$ hold, according to Descartes sign rule and Vieta theorem for univariate cubic equations, $x_1+x_2+x_3 < 0, x_1x_2x_3 > 0$, thus Eq (3.3) has two single positive root and a negative root, then the model (1.3) has two unequal positive equilibrium points $E_3^* = (x_3^*, y_3^*)$ and $E_4^* = (x_4^*, y_4^*)$, where x_3^*, x_4^* are all single positive roots and $x_3^* < x_4^*$.

(iv) When $1-(m+1)\varphi < 0$ and $(m+\lambda_1)\varphi+\gamma-(m+1) < 0$ hold, according to Descartes sign rule and Vieta theorem for univariate cubic equations, $x_1+x_2+x_3 < 0, x_1x_2x_3 > 0$, thus Eq (3.3) has a negative root and two single positive root, then we can obtain two unequal positive equilibrium points $E_5^* = (x_5^*, y_5^*), E_6^* = (x_6^*, y_6^*)$ for the model (1.3), where x_5^*, x_6^* are all single positive roots and $x_5^* < x_6^*$. Thus, when $\Delta < 0$ holds, according to Cardano formula, the model (1.3) has two single positive equilibrium points E_3^* and E_4^* or E_5^* and E_6^* under certain conditions. □

Theorem 3.2. *Based on the equilibrium point derived from Theorem 3.1 $x_1^*, x_2^*, x_3^*, x_4^*, x_5^*, x_6^*$, we can establish certain conditions that will facilitate our subsequent research endeavors: (a) $g(x_1^*) = 0$ or $g(x_2^*) = 0$; (b) $g(x_3^*) < 0$ or $g(x_5^*) < 0$; (c) $g(x_4^*) > 0$ or $g(x_6^*) > 0$.*

4. Stability of some equilibrium points

This section delves into the stability analysis of two boundary equilibrium points E_1, E_2 and some internal equilibrium points. Typically, the stability of equilibrium point can be ascertained by examining the signs of the eigenvalues at that particular point. Consequently, we present the Jacobian matrix of the model (1.3) evaluated at any equilibrium point $E(x, y)$:

$$J(x,y) = \begin{bmatrix} -3x^2+(2+2m)x-m-\frac{y+cy^2}{(1+bx+cy)^2}-\lambda_1 & -\frac{x(1+bx)}{(1+bx+cy)^2} \\ \frac{\delta y^2}{x^2} & \delta(\beta-\frac{2y}{x})-\lambda_2 \end{bmatrix},$$

utilizing the Jacobian matrix at any given point, we can formulate the following theorem.

4.1. Stability of the boundary equilibrium point

Theorem 4.1. *The stability of the boundary equilibrium point $E_2(\frac{m+1+\sqrt{(m+1)^2-4(m+\lambda_1)}}{2}, 0)$ is discussed as follows:*

1) If $\lambda_2 > \delta\beta$ holds, then the equilibrium point E_2 is a stable node.

2) If $\lambda_2 < \delta\beta$ holds, then the equilibrium point E_2 is a saddle.

3) If $\lambda_2 = \delta\beta$ holds, then the equilibrium point E_2 is a attracting saddle-node. In essence, a small enough area surrounding the equilibrium point E_2 is partitioned into two sections by two dividing lines that traverse its top and bottom, converging towards E_2 as the region diminishes. Furthermore, the left half plane comprises a parabolic sector, whereas the right half plane is comprised of two hyperbolic sectors.

Proof. We can obtain that the Jacobian matrix of the equilibrium point E_2 is:

$$J_{E_2} = \begin{bmatrix} -3x_2^2 + (2+2m)x_2 - m - \lambda_1 & -\frac{x_2}{1+bx_2} \\ 0 & \delta\beta - \lambda_2 \end{bmatrix}.$$

Apparently, J_{E_2} has two eigenvalues $\mu_1 = -3x_2^2 + (2+2m)x_2 - m - \lambda_1 = -2x_2^2 + (1+m)x_2 = -2(\frac{m+1+\sqrt{(m+1)^2-4(m+\lambda_1)}}{2})^2 + (1+m)(\frac{m+1+\sqrt{(m+1)^2-4(m+\lambda_1)}}{2}) = x_2(-\sqrt{(m+1)^2-4(m+\lambda_1)}) < 0$ and $\mu_2 = \delta\beta - \lambda_2$. Since μ_1 is consistently less than 0, it is imperative to discuss the sign of μ_2 in order to assess stability. We will approach this discussion from three distinct angles: (a) If $\mu_2 = \delta\beta - \lambda_2 < 0$, *i.e.*, $\lambda_2 > \delta\beta$, then the boundary point E_2 is a stable node. (b) If $\mu_2 = \delta\beta - \lambda_2 > 0$, *i.e.*, $\lambda_2 < \delta\beta$, then the boundary point E_2 is a saddle. (c) If $\mu_2 = \delta\beta - \lambda_2 = 0$, *i.e.*, $\lambda_2 = \delta\beta$, then the model (1.3) has two eigenvalues are $\mu_1 = x_2(-\sqrt{(m+1)^2-4(m+\lambda_1)})$ and $\mu_2 = 0$. Determining the stability of scenarios (a) and (b) is relatively straightforward. Subsequently, our focus will primarily be on scenario (c). We will shift E_2 to the origin by $(X, Y) = (x - x_2, y)$ and expand model (1.3) to the third-order using Taylor's series, obtaining:

$$\begin{cases} \dot{X} = & \alpha_{10}X + \alpha_{01}Y + \alpha_{11}XY + \alpha_{20}X^2 + \alpha_{02}Y^2 + \alpha_{30}X^3 \\ & +\alpha_{21}X^2Y + \alpha_{12}XY^2 + \alpha_{03}Y^3 + M_1(X,Y), \\ \dot{Y} = & -\delta Y^2 + \delta XY^2 + N_1(X,Y), \end{cases} \tag{4.1}$$

where $\alpha_{10} = -3x_2{}^2 + 2(1+m)x_2 - (m+\lambda_1)$, $\alpha_{01} = -\frac{x_2(1+bx_2)}{(1+bx_2)^2}$, $\alpha_{02} = \frac{cx_2}{(1+bx_2)^2}$, $\alpha_{11} = -\frac{1}{(1+bx_2)^2}$, $\alpha_{20} = -3x_2 + 1 + m$, $\alpha_{30} = -1$, $\alpha_{03} = -\frac{c^2x_2}{(1+bx_2)^3}$, $\alpha_{21} = \frac{b}{(1+bx_2)^3}$, $\alpha_{12} = -\frac{c(bx_2-1)}{(1+bx_2)^3}$, and $M_1(X,Y)$, $N_1(X,Y)$ are fourth-order infinitesimal quantity.

By the simplistic transformation

$$\begin{pmatrix} X \\ Y \end{pmatrix} = \begin{pmatrix} 1 & -\frac{\alpha_{01}}{\alpha_{10}} \\ 0 & 1 \end{pmatrix} \begin{pmatrix} x \\ y \end{pmatrix},$$

then

$$\begin{cases} X = x - \frac{\alpha_{01}}{\alpha_{10}}y, \\ Y = y, \end{cases}$$

where $\alpha_{10} = -3x_2{}^2 + 2(1+m)x_2 - (m+\lambda_1)$, $\alpha_{01} = -\frac{x_2(1+bx_2)}{(1+bx_2)^2}$.

Thus, the model (4.1) becomes a standard form

$$\begin{cases} \dot{x} = & \alpha_{10}X + \alpha_{20}X^2 + h_1XY + h_2Y^2 + h_3X^3 \\ & +h_4X^2Y + h_5XY^2 + h_6Y^3 + M_2(X,Y), \\ \dot{y} = & -\delta y^2 + \delta xy^2 - \frac{\alpha_{01}}{\alpha_{10}}y^3 + N_2(X,Y), \end{cases} \tag{4.2}$$

where $\alpha_{10} = -3x_2{}^2 + 2(1+m)x_2 - (m+\lambda_1)$, $\alpha_{01} = -\frac{x_2(1+bx_2)}{(1+bx_2)^2}$, $h_1 = \alpha_{20}\frac{-2\alpha_{01}}{\alpha_{10}} + \alpha_{11}$, $h_2 = \alpha_{20}(\frac{\alpha_{01}}{\alpha_{10}})^2 - \frac{\alpha_{11}\alpha_{01}}{\alpha_{10}} + \alpha_{02}$, $M_2(x,y)$ and $N_2(x,y)$ are fourth-order infinitesimal quantity, and the remaining algorithms of h_3, h_4, h_5, h_6

are the same, so we will not list them one by one here. Since the coefficient of y^2 for the second equation of the model (4.2) is $-\delta < 0$, the key internal point $E_2(\frac{m+1+\sqrt{(m+1)^2-4(m+\lambda_1)}}{2}, 0)$ is a attracting saddle-node if $\lambda_2 = \delta\beta$. Thus we can obtained this results from Theorem 7.1 in Chapter 2 in [49]. □

Furthermore, it is easy to obtain that the boundary equilibrium point $E_1(\frac{m+1-\sqrt{(m+1)^2-4(m+\lambda_1)}}{2}, 0)$ is a saddle if $\lambda_2 > \delta\beta$, is an unstable node if $\lambda_2 < \delta\beta$, and is a saddle-node if $\lambda_2 = \delta\beta$.

4.2. Stability of some internal equilibrium points

We will delve into the stability of some internal equilibrium points, echoing the discussions presented in Section 4.1. Specifically, we will proceed to compute the Jacobian matrix for any given internal equilibrium point as follows:

$$J_{E^*} = \begin{bmatrix} -3x^{*2} + (2+2m)x^* - m - \frac{(\beta-\frac{\lambda_2}{\delta})x^* + c((\beta-\frac{\lambda_2}{\delta})x^*)^2}{(1+bx^*+c(\beta-\frac{\lambda_2}{\delta})x^*)^2} - \lambda_1 & -\frac{x^*(1+bx^*)}{(1+bx^*+c(\beta-\frac{\lambda_2}{\delta})x^*)^2} \\ (\beta-\frac{\lambda_2}{\delta})^2\delta & \lambda_2 - \delta\beta \end{bmatrix},$$

then we get:

$$\begin{aligned} Det(J_{E^*}) &= (-3x^{*2} + (2+2m)x^* - m - \frac{\gamma x^* + c(\gamma x^*)^2}{(1+bx^*+c\gamma x^*)^2} - \lambda_1)(\lambda_2 - \delta\beta) - (-\frac{x^*(1+bx^*)}{(1+\varphi x^*)^2})(\gamma^2\delta) \\ &= -(\beta - \frac{\lambda_2}{\delta})\delta(\frac{2\varphi x^{*3} + (1-(1+m)\varphi)x^{*2} - m - \lambda_1}{1+\varphi x^*}) \\ &= -(\beta - \frac{\lambda_2}{\delta})\delta(\frac{T_1 x^{*2} + 2T_2 x^* + 3(m+\lambda_1)}{1+\varphi x^*}) \\ &= \frac{(\beta-\frac{\lambda_2}{\delta})\delta x^*}{1+\varphi x^*}(3\varphi x^{*2} + 2T_1 x + T_2) \\ &= (\beta - \frac{\lambda_2}{\delta})\delta x^*(\frac{T_1 x^{*2} + 2T_2 x^* + 3(m+\lambda_1)}{1+\varphi x^*}) \\ &= \frac{(\beta-\frac{\lambda_2}{\delta})\delta x^*}{1+\varphi x^*}(f(x^*)'), \\ Tr(J_{E^*}) &= -3x^{*2} + (2+2m)x^* - m - \frac{(\beta-\frac{\lambda_2}{\delta})x^* + c((\beta-\frac{\lambda_2}{\delta})x^*)^2}{(1+bx^*+c(\beta-\frac{\lambda_2}{\delta})x^*)^2} - \lambda_1 + \lambda_2 - \delta\beta. \end{aligned}$$

4.2.1. Stability of the equilibrium points E_1^* and E_2^*

Lemma 4.1. *([49]). The model*

$$\begin{cases} \dot{\alpha} = \beta + A\alpha^2 + B\alpha\beta + C\beta^2 + M_1(\alpha,\beta), \\ \dot{\beta} = D\alpha^2 + E\alpha\beta + F\beta^2 + N_1(\alpha,\beta), \end{cases} \tag{4.3}$$

where $M_1(\alpha,\beta)$ and $N_1(\alpha,\beta)$ are tired-order infinitesimal quantity, i.e., $M_1(\alpha,\beta) = o(|\alpha,\beta|^2)$, $N_1(\alpha,\beta) = o(|\alpha,\beta|^2)$, we can transform Eq (4.3) into (4.4)

$$\begin{cases} \dot{\alpha} = \beta, \\ \dot{\beta} = D\alpha^2 + (E + 2F)\alpha\beta + o(|\alpha,\beta|^2), \end{cases} \tag{4.4}$$

by certain nonsingular transformations in the domain of $(0, 0)$.

Theorem 4.2. *If $\Delta = 0, 1 - (m + 1)\varphi > 0$ and $(m + \lambda_1)\varphi + \gamma - (m + 1) < 0$ hold, then the model (1.3) has an internal point $E_1^* = (x_1^*, y_1^*)$, where x_1^* is a dual root, then:*

1) If $m \neq -3x_1^{*2} + (2 + 2m)x_1^* - \frac{(\beta-\frac{\lambda_2}{\delta})x_1^* + c((\beta-\frac{\lambda_2}{\delta})x_1^*)^2}{(1+bx_1^*+c(\beta-\frac{\lambda_2}{\delta})x_1^*)^2} - \lambda_1 + \lambda_2 - \delta\beta$ and $m \neq 3x_1^* - 1 + \frac{\beta-\frac{\lambda_2}{\delta}}{(1+bx_1^*+c(\beta-\frac{\lambda_2}{\delta})x_1^*)^3}$ hold, then the internal point E_1^* is a saddle-node.

2) If $m = -3x_1^{*2} + (2 + 2m)x_1^* - \frac{(\beta-\frac{\lambda_2}{\delta})x_1^* + c((\beta-\frac{\lambda_2}{\delta})x_1^*)^2}{(1+bx_1^*+c(\beta-\frac{\lambda_2}{\delta})x_1^*)^2} - \lambda_1 + \lambda_2 - \delta\beta$ holds, the internal point E_1^* is a cusp. Further, if $m \neq 3x_1^* - 1 + \frac{\beta-\frac{\lambda_2}{\delta}}{(1+bx_1^*+c(\beta-\frac{\lambda_2}{\delta})x_1^*)^3}$ and $m \neq 3x_1^* - 1 + \frac{(\beta-\frac{\lambda_2}{\delta})-(\beta-\frac{\lambda_2}{\delta})bx_1^*+(\beta-\frac{\lambda_2}{\delta})cy_1^*}{2(1+bx_1^*+c(\beta-\frac{\lambda_2}{\delta})x_1^*)^3}$ hold, then the internal point E_1^* is a cusp with codimension 2. If $m = 3x_1^* - 1 + \frac{\beta-\frac{\lambda_2}{\delta}}{(1+bx_1^*+c(\beta-\frac{\lambda_2}{\delta})x_1^*)^3}$ or $m = 3x_1^* - 1 + \frac{(\beta-\frac{\lambda_2}{\delta})-(\beta-\frac{\lambda_2}{\delta})bx_1^*+(\beta-\frac{\lambda_2}{\delta})cy_1^*}{2(1+bx_1^*+c(\beta-\frac{\lambda_2}{\delta})x_1^*)^3}$ hold, then the internal point E_1^* is a cusp with codimension at least 3.

Proof. Firstly, we utilize the approach outlined in Lemma 4.1 to shift the origin to E_1^* by setting $(X, Y) = (x - x_1^*, y - y_1^*)$ and derive a new model (4.5) accordingly:

$$\begin{cases} \dot{X} = q'_{10}X + q'_{01}Y + q'_{20}X^2 + q'_{11}XY + q'_{02}Y^2 + M_3(X, Y), \\ \dot{Y} = p'_{10}X + p'_{01}Y + p'_{20}X^2 + p'_{11}XY + p'_{02}Y^2 + N_3(X, Y), \end{cases} \tag{4.5}$$

where

$$q'_{10} = -3x_1^{*2} + 2(1 + m)x_1^* - (m + \lambda_1) - \frac{y_1^*(1 + cy_1^*)}{(1 + bx_1^* + cy_1^*)^2}, \quad q'_{01} = -\frac{x_1^*(1 + bx_1^*)}{(1 + bx_1^* + cy_1^*)^2},$$

$$q'_{11} = -\frac{1}{(1 + bx_1^* + cy_1^*)^2} - \frac{2bcx_1^*y_1^*}{(1 + bx_1^* + cy_1^*)^3}, \quad q'_{20} = -3x_1^* + 1 + m + \frac{by_1^*(1 + cy_1^*)}{(1 + bx_1^* + cy_1^*)^3},$$

$$q'_{02} = \frac{cx_1^*(1 + bx_1^*)}{(1 + bx_1^* + cy_1^*)^3}, \quad p'_{10} = \frac{\delta y_1^{*2}}{x_1^{*2}}, \quad p'_{01} = \delta(\beta - \frac{2y_1^*}{x_1^*}) - \lambda_2,$$

$$p'_{11} = \frac{2\delta y_1^*}{x_1^{*2}}, \quad p'_{20} = -\frac{\delta y_1^{*2}}{x_1^{*3}}, \quad p'_{02} = -\frac{\delta}{x_1^*},$$

and $M_3(X, Y)$, $N_3(X, Y)$ are third-order infinitesimal quantity.

Case 1: $m \neq -3x_1^{*2} + (2 + 2m)x_1^* - \frac{(\beta-\frac{\lambda_2}{\delta})x_1^* + c((\beta-\frac{\lambda_2}{\delta})x_1^*)^2}{(1+bx_1^*+c(\beta-\frac{\lambda_2}{\delta})x_1^*)^2} - \lambda_1 + \lambda_2 - \delta\beta$.

In this scenario, the Jacobian matrix of the model (4.5) is presented as follows:

$$J_{E_1^*} = \begin{pmatrix} q'_{10} & -\frac{q'_{10}}{\beta-\frac{\lambda_2}{\delta}} \\ -(\beta - \frac{\lambda_2}{\delta})p'_{01} & p'_{01} \end{pmatrix},$$

then we can get that $\mu_1 = 0$, $\mu_2 = q'_{10} + p'_{01}$ are two eigenvalues of $J_{E_1^*}$. By a transformation, we can transform the model (4.5) into the model (4.6):

$$\begin{pmatrix} X \\ Y \end{pmatrix} = \begin{pmatrix} q'_{10} & 1 \\ \delta(\beta - \frac{\lambda_2}{\delta})^2 & \beta - \frac{\lambda_2}{\delta} \end{pmatrix} \begin{pmatrix} x \\ y \end{pmatrix}.$$

After that, the model (4.5) becomes

$$\begin{cases} \dot{x} = (q'_{10} + \lambda_2 - \delta\beta)x + w'_{20}x^2 + w'_{11}xy + w'_{02}y^2 + M_4(x, y), \\ \dot{y} = z'_{20}x^2 + z'_{11}xy + z'_{02}y^2 + N_4(x, y), \end{cases} \tag{4.6}$$

where

$$\begin{aligned}
w'_{20} &= -\frac{\gamma^5\delta^2 q'_{02} - p'_{02}\delta^2\gamma^4 + \gamma^3\delta q'_{10}q'_{11} - p'_{11}q'_{10}\delta\gamma^2 + \gamma q'^2_{10}q'_{20} - p'_{20}q'^2_{10}}{\gamma\left(\delta\gamma - q'_{10}\right)}, \\
w'_{11} &= -\frac{2\gamma^4\delta q'_{02} + \gamma^3\delta q'_{11} - 2\gamma^3\delta p'_{02} - \gamma^2\delta p'_{11} + \gamma^2 q'_{10}q'_{11} + 2\gamma q'_{10}q'_{20} - \gamma q'_{10}p'_{11} - 2q'_{10}p'_{20}}{\gamma\left(\delta\gamma - q'_{10}\right)}, \\
w'_{02} &= -\frac{\gamma^3 q'_{02} + \gamma^2 q'_{11} - p'_{02}\gamma^2 + \gamma q'_{20} - p'_{11}\gamma - p'_{20}}{\gamma\left(\delta\gamma - q'_{10}\right)}, \\
z'_{11} &= \frac{2\gamma^5\delta^2 q'_{02} + \gamma^4\delta^2 q'_{11} + \gamma^3\delta q'_{10}q'_{11} - 2\gamma^3\delta q'_{10}p'_{02} + 2\gamma^2\delta q'_{10}q'_{20} - p'_{11}q'_{10}\delta\gamma^2 - \gamma q'^2_{10}p'_{11} - 2p'_{20}q'^2_{10}}{\gamma\left(\delta\gamma - q'_{10}\right)}, \\
z'_{20} &= \frac{\gamma^6\delta^3 q'_{02} + \gamma^4\delta^2 q'_{10}q'_{11} - \gamma^4\delta^2 q'_{10}p'_{02} + \gamma^2\delta q'^2_{10}q'_{20} - \gamma^2\delta q'^2_{10}p'_{11} - q'^3_{10}p'_{20}}{\gamma\left(\delta\gamma - q'_{10}\right)}, \\
z'_{02} &= \frac{\gamma^4\delta q'_{02} + \gamma^3\delta q'_{11} + \gamma^2\delta q'_{20} - \gamma^2 q'_{10}p'_{02} - \gamma q'_{10}p'_{11} - q'_{10}p'_{20}}{\gamma\left(\delta\gamma - q'_{10}\right)},
\end{aligned}$$

and $\gamma = \beta - \frac{\lambda_2}{\delta}$, $M_4(x, y)$, $N_4(x, y)$ are third-order infinitesimal quantity.

We introduce a new transformation ι to the model (4.7) by $\iota = (q'_{10} + \lambda_2 - \delta\beta)t$, and continue to use t as a substitute for ι, and upon substitution, thus we can obtain the following model (4.7):

$$\begin{cases} \dot{x} = x + r'_{20}x^2 + r'_{11}xy + r'_{02}y^2 + M_5(x, y), \\ \dot{y} = s'_{20}x^2 + s'_{11}xy + s'_{02}y^2 + N_5(x, y), \end{cases} \tag{4.7}$$

where $r'_{ij} = \frac{w'_{ij}}{q'_{10}+\lambda_2-\delta\beta}$, $s'_{ij} = \frac{z'_{ij}}{q'_{10}+\lambda_2-\delta\beta}$ $(i + j = 2)$, $M_5(x, y)$, $N_5(x, y)$ are third-order infinitesimal quantity.

Then we can obtain

$$\begin{aligned}
z'_{02} &= \frac{\gamma^4\delta q'_{02} + \gamma^3\delta q'_{11} + \gamma^2\delta q'_{20} - \gamma^2 q'_{10}p'_{02} - \gamma q'_{10}p'_{11} - q'_{10}p'_{20}}{\gamma\left(\delta\gamma - q'_{10}\right)} \\
&= \frac{\gamma^4\delta\frac{cx_1^*(1+bx_1^*)}{T_3^3} + \gamma^3\delta(-\frac{1}{T_3^2} - \frac{2bcx_1^*y_1^*}{T_3^3}) + \gamma^2\delta(-3x_1^* + 1 + m + \frac{by_1^*(1+cy_1^*)}{T_3^3}) - \gamma^2 q'_{10}(\frac{\delta}{x_1^*} - \frac{2\delta}{x_1^*} + \frac{\delta}{x_1^*})}{\gamma\left(\delta\gamma - (-3x_1^{*2} + 2(1 + m)x_1^* - (m + \lambda_1) - \frac{y_1^*(1+cy_1^*)}{T_3^2})\right)}
\end{aligned}$$

$$= \frac{\gamma^2\delta[\frac{\gamma^2cx_1^*+\gamma^2bcx_1^{*2}-\gamma^2(1+bx_1^*+cy_1^*)-2\gamma^2bcx_1^{*2}+\gamma bx_1^*+\gamma^2bcx_1^{*2}}{T_3^3} - 3x_1^* + 1 + m]}{\gamma\left(\delta\gamma - (-3x_1^{*2} + 2(1+m)x_1^* - (m+\lambda_1) - \frac{y_1^*(1+cy_1^*)}{T_3^2})\right)}$$

$$= \frac{\gamma\delta(\frac{-\gamma}{T_3^3} - 3x_1^* + 1 + m)}{\delta\gamma - (-3x_1^{*2} + 2(1+m)x_1^* - (m+\lambda_1) - \frac{y_1^*(1+cy_1^*)}{T_3^2})},$$

and

$$s'_{02} = \frac{z'_{02}}{q'_{10} + \lambda_2 - \delta\beta}.$$

According to [49] , we can determine that E_1^* is a saddle-node if $z'_{02} \neq 0$ and $s'_{02} \neq 0$. That is, if

$$\gamma\delta(\frac{-\gamma}{T_3^3} - 3x_1^* + 1 + m) \neq 0,$$

i.e.,

$$m \neq 3x_1^* - 1 + \frac{\beta - \frac{\lambda_2}{\delta}}{(1 + bx_1^* + c(\beta - \frac{\lambda_2}{\delta})x_1^*)^3},$$

and

$$\delta\gamma - (-3x_1^{*2} + 2(1+m)x_1^* - (m+\lambda_1) - \frac{y_1^*(1+cy_1^*)}{T_3^2}) \neq 0,$$

i.e.,

$$m \neq -3x_1^{*2} + (2+2m)x_1^* - \frac{(\beta - \frac{\lambda_2}{\delta})x_1^* + c((\beta - \frac{\lambda_2}{\delta})x_1^*)^2}{(1 + bx_1^* + c(\beta - \frac{\lambda_2}{\delta})x_1^*)^2} - \lambda_1 + \lambda_2 - \delta\beta.$$

Case 2: $m = -3x_1^{*2} + (2+2m)x_1^* - \frac{(\beta - \frac{\lambda_2}{\delta})x_1^* + c((\beta - \frac{\lambda_2}{\delta})x_1^*)^2}{(1 + bx_1^* + c(\beta - \frac{\lambda_2}{\delta})x_1^*)^2} - \lambda_1 + \lambda_2 - \delta\beta.$

A new Jacobi matrix of the model (4.5) is

$$J_{E_1^*} = \begin{pmatrix} q'_{10} & -\frac{q'_{10}}{\beta - \frac{\lambda_2}{\delta}} \\ (\beta - \frac{\lambda_2}{\delta})q'_{10} & -q'_{10} \end{pmatrix},$$

then we can get that $\mu_1 = 0, \mu_2 = 0$ are two eigenvalues of $J_{E_1^*}$. By a transformation, we can transform the model (4.5) into (4.8)

$$\begin{pmatrix} X \\ Y \end{pmatrix} = \begin{pmatrix} 1 & 0 \\ \beta - \frac{\lambda_2}{\delta} & -1 \end{pmatrix} \begin{pmatrix} x \\ y \end{pmatrix}.$$

After that, the model (4.5) becomes

$$\begin{cases} \dot{x} = \delta y + w_{20}x^2 + w_{11}xy + w_{02}y^2 + M_6(x,y), \\ \dot{y} = z_{20}x^2 + z_{11}xy + z_{02}y^2 + N_6(x,y), \end{cases} \tag{4.8}$$

where

$$w_{20} = q'_{02}\gamma^2 + \gamma q'_{11} + q'_{20}, \quad w_{11} = -2\gamma q'_{02} - q'_{11}, \quad w_{02} = q'_{02}, \quad z_{02} = \gamma q'_{02} - p'_{02}$$
$$z_{11} = 2\gamma p'_{02} + p'_{11} - 2q'_{02}\gamma^2 - \gamma q'_{11}, \quad z_{20} = \gamma^3 q'_{02} + \gamma^2(q'_{11} - p'_{02}) + \gamma(q'_{20} - p'_{11}) - p'_{20},$$

and $\gamma = \beta - \frac{\lambda_2}{\delta}$, $M_6(x, y)$, $N_6(x, y)$ are third-order infinitesimal quantity.

We introduce a new transformation ι to the model (4.9) by $\iota = \delta t$, and continue to use t as a substitute for ι, hence we can obtain the following model (4.9):

$$\begin{cases} \dot{x} = y + r_{20}x^2 + r_{11}xy + r_{02}y^2 + M_7(x, y), \\ \dot{y} = s_{20}x^2 + s_{11}xy + s_{02}y^2 + N_7(x, y), \end{cases} \tag{4.9}$$

where $r_{ij} = \frac{w_{ij}}{\delta}$, $s_{ij} = \frac{z_{ij}}{\delta}$ $(i + j = 2)$, $M_7(x, y)$, $N_7(x, y)$ are third-order infinitesimal quantity.

According to [49] , we can determine that E_1^* is a cusp. Let us make the next deffnitions

$$A(x, y) \triangleq r_{20}x^2 + r_{11}xy + r_{02}y^2 + M_7(x, y), \quad B(x, y) \triangleq s_{20}x^2 + s_{11}xy + s_{02}y^2 + N_7(x, y).$$

We can get $y + A(x, y) = 0$ and $r_{20} \neq 0$, and also we can obtain

$$y = \chi(x) = -r_{20}x^2 + \cdots,$$

then we have

$$\psi(x) \triangleq B(x, \chi(x)) = S_{20}x^2 + \cdots, \quad \omega(x) \triangleq \frac{\partial A}{\partial x}(x, \chi(x)) + \frac{\partial B}{\partial y}(x, \chi(x)) = (2r_{20} + s_{11})x + \cdots.$$

According to Lemma 4.1, we can transform the model (4.9) into (4.10)

$$\begin{cases} \dot{x} = y, \\ \dot{y} = s_{20}x^2 + (s_{11} + 2r_{20})xy + N_8(x, y), \end{cases} \tag{4.10}$$

where $N_8(x, y)$ is third-order infinitesimal quantity.

Then we can obtain

$$\begin{aligned}
s_{20} &= \frac{z_{20}}{\delta} = \frac{\gamma^3 q'_{02} + \gamma^2(q'_{11} - p'_{02}) + \gamma(q'_{20} - p'_{11}) - p'_{20}}{\delta} \\
&= \frac{\gamma}{\delta}\left[\gamma^2\left(\frac{wx_1^*(1 + px_1^*)}{T_3^3}\right) + \gamma\left(-\frac{1}{T_3^2} - \frac{2bcx_1^*y_1^*}{T_3^3} + \frac{\delta}{x_1^*}\right) - 3x_1^* + 1 + m + \frac{by_1^*(1 + cy_1^*)}{T_3^3} - \frac{2\delta y_1^*}{x_1^{*2}} + \frac{\delta\gamma}{x_1^*}\right] \\
&= \frac{\gamma}{\delta}\left[\frac{-\gamma}{T_3^3} - 3x_1^* + 1 + m\right], \\
s_{11} &= \frac{z_{11}}{\delta} = \frac{2\gamma p'_{02} + p'_{11} - 2q'_{02}\gamma^2 - \gamma q'_{11}}{\delta} \\
&= \frac{\gamma}{\delta}\left[-2\frac{\delta}{x_1^*} + \frac{2\delta}{x_1^*} - 2\frac{cx_1^*(1 + bx_1^*)}{T_3^3}\gamma - \left(-\frac{1}{T_3^2} - \frac{2bcx_1^*y_1^*}{T_3^3}\right)\right] \\
&= \frac{\gamma}{\delta}\left[\frac{1 + bx_1^* - c\gamma x_1^*}{T_3^3}\right], \\
r_{20} &= \frac{w_{20}}{\delta} = \frac{q'_{02}\gamma^2 + \gamma q'_{11} + q'_{20}}{\delta} \\
&= \frac{1}{\delta}\left[\frac{cx_1^*(1 + bx_1^*)}{T_3^3}\gamma^2 + \gamma\left(-\frac{1}{T_3^2} - \frac{2bcx_1^*y_1^*}{T_3^3}\right) - 3x_1^* + 1 + m + \frac{by_1^*(1 + cy_1^*)}{T_3^3}\right]
\end{aligned}$$

$$= \frac{1}{\delta}\left[\frac{-\gamma}{T_3^3} - 3x_1^* + 1 + m\right],$$

where $T_3 = 1 + bx_1^* + cy_1^*$. Therefore, according to [49], we can determine that E_1^* is a cusp when $k = 2h, h = 1, q_{2m} = s_{20}, N = 1, B_N = 2r_{20} + s_{11}$. Furthermore, if $s_{20} \neq 0$ and $s_{11} + 2r_{20} \neq 0$, then the internal point E_1^* is a cusp with codimension 2. If $s_{02} = 0$ or $s_{11} + 2r_{20} = 0$, then the internal point E_1^* is a cusp with codimension at least 3. That is

$$\begin{aligned} s_{11} + 2r_{20} &= \frac{\gamma^3 q'_{02} + \gamma^2(q'_{11} - p'_{02}) + \gamma(q'_{20} - p'_{11}) - p'_{20}}{\delta} + \frac{2(q'_{02}\gamma^2 + \gamma q'_{11} + q'_{20})}{\delta} \\ &= \frac{\gamma}{\delta}\left(\frac{1 + bx_1^* - c\gamma x_1^*}{T_3^3}\right) + \frac{2}{\delta}\left(\frac{-\gamma}{T_3^3} - 3x_1^* + 1 + m\right) \\ &= \frac{1}{\delta}\left(\frac{-\gamma - \gamma b x_1^* - \gamma c y_1^* - 2\gamma b c x_1^* y_1^* + 2b y_1^* + 2b c y_1^{*2}}{T_3^3} - 6x_1^* + 2 + 2m\right) \\ &= \frac{1}{\delta}\left(\frac{-\gamma + \gamma b x_1^* - \gamma c y_1^*}{T_3^3} - 6x_1^* + 2 + 2m\right) \neq 0, \end{aligned}$$

i.e.,

$$m \neq 3x_1^* - 1 + \frac{(\beta - \frac{\lambda_2}{\delta}) - (\beta - \frac{\lambda_2}{\delta})bx_1^* + (\beta - \frac{\lambda_2}{\delta})cy_1^*}{2(1 + bx_1^* + c(\beta - \frac{\lambda_2}{\delta})x_1^*)^3}.$$

□

Otherwise, when $\Delta = 0$, $1 - (m+1)\varphi < 0$ and $(m + \lambda_1)\varphi + \gamma - (m+1) < 0$ hold, the stability investigation of the internal point E_2^* is similar to the discussion of stability of the equilibrium point E_1^*, so we simply ignore it.

4.2.2. Stability of the equilibrium point E_i^*

If the conditions for the existence of equilibrium points E_i^* $(i = 3, 4, 5, 6,)$ are satisfied, the values of $Det(J_{E_3^*})$ and $Det(J_{E_5^*})$ are consistently negative,

$$Det(J_{E^*}) = \frac{(\beta - \frac{\lambda_2}{\delta})\delta x^*}{1 + \varphi x^*}(f(x^*)').$$

Therefore, as their determinants are consistently less than 0 by Theorem 3.2, the equilibrium points E_3^* and E_5^* are classified as saddle. Pursuant to Theorem 3.2, it is ascertainable that the values of $Det(J_{E_4^*})$ and $Det(J_{E_6^*})$ remain positive at all times. Subsequently, our discussion shall encompass three perspectives: (a) If $Tr(J_{E_i^*}) > 0$, it is a source. (b) If $Tr(J_{E_i^*}) = 0$, it is a center. (c) If $Tr(J_{E_i^*}) < 0$, it is a sink.

Hence, we can consolidate the aforementioned analysis and gain the following theorem.

Theorem 4.3. *Pursuant to Theorem 3.2, it is ascertainable that the values of $Det(J_{E_4^*})$ and $Det(J_{E_6^*})$ remain positive at all times. Subsequently, our discussion shall encompass three perspectives: (a) If $Tr(J_{E_i^*}) > 0$, it is a source. (b) If $Tr(J_{E_i^*}) = 0$, it is a center. (c) If $Tr(J_{E_i^*}) < 0$, it is a sink.*

Theorem 4.4. *Therefore, as their determinants are consistently less than 0 by Theorem 3.2, the equilibrium points E_3^* and E_5^* are classified as saddle.*

5. Bifurcation analysis

To investigate the impact of Allee effect and harvesting effort on the dynamic behavior of the model (1.3), we chose λ_2 and m as bifurcation control parameters and encompassed transcritical bifurcation, saddle-node bifurcation, Hopf bifurcation, and Bogdanov-Takens bifurcation of the model (1.3).

5.1. Transcritical bifurcation

Theorem 5.1. *The model (1.3) can undergo a transcritical bifurcation when $\lambda_2 = \lambda_{TC} = \beta\delta$.*

Proof. When $\lambda_2 = \lambda_{TC} = \beta\delta$, we can get the Jacobian matrix from Theorem 4.1:

$$J_{E_2} = \begin{pmatrix} x_2(-2x_2 + 1 + m) & -\frac{x_2}{1+bx_2} \\ 0 & 0 \end{pmatrix}.$$

Next, we demonstrate the occurrence of transcritical bifurcation by the Sotomayor's theorem. Assuming that U represents the eigenvector of J_{E_2} pertaining to 0, and V corresponds to the eigenvector of $J_{E_2}^T$ pertaining to 0, we present the following exposition:

$$U = \begin{pmatrix} u_1 \\ u_2 \end{pmatrix} = \begin{pmatrix} \frac{x_2}{1+bx_2} \\ x_2(-2x_2 + 1 + m) \end{pmatrix}, \qquad V = \begin{pmatrix} v_1 \\ v_2 \end{pmatrix} = \begin{pmatrix} 0 \\ 1 \end{pmatrix}.$$

Then we can get

$$F_{\lambda_2}(E_2; \lambda_{TC}) = \begin{pmatrix} 0 \\ -y \end{pmatrix}_{(E_2;\lambda_{TC})} = \begin{pmatrix} 0 \\ 0 \end{pmatrix},$$

$$DF_{\lambda_2}(E_2; \lambda_{TC})U = \begin{pmatrix} 0 & 0 \\ 0 & -1 \end{pmatrix}\begin{pmatrix} \frac{x_2}{1+bx_2} \\ x_2(-2x_2 + 1 + m) \end{pmatrix} = \begin{pmatrix} 0 \\ x_2(2x_2 - 1 - m) \end{pmatrix},$$

$$D^2F_{\lambda_2}(E_2; \lambda_{TC})(U, U) = \begin{pmatrix} \frac{\partial^2 F_1}{\partial x^2}u_1u_1 + 2\frac{\partial^2 F_1}{\partial x\partial y}u_1u_2 + \frac{\partial^2 F_1}{\partial y^2}u_2u_2 \\ \frac{\partial^2 F_2}{\partial x^2}u_1u_1 + 2\frac{\partial^2 F_2}{\partial x\partial y}u_1u_2 + \frac{\partial^2 F_2}{\partial y^2}u_2u_2 \end{pmatrix}_{(E_2;\lambda_{TC})}$$

$$= \begin{pmatrix} (-4x_2 + m + 1)(\frac{x_2}{1+bx_2})^2 + \frac{1}{(1+bx_2)^2}x_2(-2x_2 + 1 + m)\frac{x_2}{1+bx_2} \\ -\frac{2\delta}{x_2}[x_2(-2x_2 + 1 + m)]^2 \end{pmatrix}$$

$$= \begin{pmatrix} -4bx_2^4 + (bm + b - 6)x_2^3 + 2(m + 1)x_2^2 \\ -\frac{2\delta}{x_2}[x_2(-2x_2 + 1 + m)]^2 \end{pmatrix}.$$

Therefore, we can get

$$V^T F_{\lambda_2}(E_2; \lambda_{TC}) = 0,$$

$$V^T[DF_{\lambda_2}(E_2; \lambda_{TC})U] = x_2(2x_2 - 1 - m) \neq 0,$$

$$V^T[D^2F_{\lambda_2}(E_2; \lambda_{TC})(U, U)] = -\frac{2\delta}{x_2}[x_2(-2x_2 + 1 + m)]^2 \neq 0.$$

Therefore, the model (1.3) can undergo a transcritical bifurcation when $\lambda_2 = \lambda_{TC} = \beta\delta$. □

5.2. Saddle-node bifurcation

According to the Theorem 3.1 Case 3, we can get a bifurcation surface for saddle-node:

$$SN = \left\{(m, b, c, \beta, \delta, \lambda_1, \lambda_2) : \beta - \frac{\lambda_2}{\delta} > 0, \Delta = 0, T_1 < 0, T_2 > 0\right\},$$

where $T_1 = 1 - (m+1)[b + c(\beta - \frac{\lambda_2}{\delta})]$ and $T_2 = (m+\lambda_1)[b + c(\beta - \frac{\lambda_2}{\delta})] + \beta - \frac{\lambda_2}{\delta} - (m+1)$.

We can observe that the sign of Δ can be altered by λ_2, during which process the number of equilibrium points transforms from 0 to 1 and then to 2. Consequently, to ascertain whether the model (1.3) is capable of undergoing a saddle-node bifurcation, we proceed with the following derivation.

Theorem 5.2. *Under the condition of:*
1) $\beta - \frac{\lambda_2}{\delta} > 0$,
2) $1 - (m+1)[b + c(\beta - \frac{\lambda_2}{\delta})] < 0$,
3) $(m+\lambda_1)[b + c(\beta - \frac{\lambda_2}{\delta})] + \beta - \frac{\lambda_2}{\delta} - (m+1) > 0$,
when $\Delta = 0$, *i.e.,* $\lambda_2 = \lambda_{SN}$, *the model (1.3) can undergo a saddle-node bifurcation.*

Proof. Now, we demonstrate the occurrence of transcritical bifurcation by the Sotomayor's theorem, the Jacobian matrix at E_1^* is:

$$J_{E_1^*} = \begin{bmatrix} -3{x_1^*}^2 + (2+2m)x_1^* - m - \frac{(\beta-\frac{\lambda_2}{\delta})x_1^* + c((\beta-\frac{\lambda_2}{\delta})x_1^*)^2}{(1+bx_1^*+c(\beta-\frac{\lambda_2}{\delta})x_1^*)^2} - \lambda_1 & -\frac{x_1^*(1+bx_1^*)}{(1+bx_1^*+c(\beta-\frac{\lambda_2}{\delta})x_1^*)^2} \\ (\beta-\frac{\lambda_2}{\delta})^2\delta & \lambda_2 - \delta\beta \end{bmatrix}.$$

If $\lambda_2 = \lambda_{SN}$, the Jacobian matrix at E_1^* can be written in the following form:

$$J_{E_1^*} = \begin{pmatrix} -e_{12}\gamma & e_{12} \\ \delta\gamma^2 & -\delta\gamma \end{pmatrix},$$

where $\gamma = \beta - \frac{\lambda_{SN}}{\delta}$, $e_{12} = -\frac{x_1^*(1+bx_1^*)}{(1+bx_1^*+c(\beta-\frac{\lambda_2}{\delta}))^2}$.

Zero is one of the eigenvalues, then we can assume that U represents the eigenvector of $J_{E_1^*}$ pertaining to 0, and V corresponds to the eigenvector of $J_{E_1^*}^T$ pertaining to 0, we present the following exposition:

$$U = \begin{pmatrix} u_1 \\ u_2 \end{pmatrix} = \begin{pmatrix} 1 \\ \gamma \end{pmatrix}, \qquad V = \begin{pmatrix} v_1 \\ v_2 \end{pmatrix} = \begin{pmatrix} \frac{\delta\gamma}{a_{12}} \\ 1 \end{pmatrix}.$$

Therefore, we can obtain

$$\begin{aligned} F_{\lambda_2}(E_1^*; \lambda_{SN}) &= \begin{pmatrix} 0 \\ -y \end{pmatrix}_{(E_1^*;\lambda_{SN})} = \begin{pmatrix} 0 \\ -y_1^* \end{pmatrix}, \\ D^2F(E_1^*; \lambda_{SN})(U,U) &= \begin{pmatrix} \frac{\partial^2 F_1}{\partial x^2}u_1u_1 + 2\frac{\partial^2 F_1}{\partial x\partial y}u_1u_2 + \frac{\partial^2 F_1}{\partial y^2}u_2u_2 \\ \frac{\partial^2 F_2}{\partial x^2}u_1u_1 + 2\frac{\partial^2 F_2}{\partial x\partial y}u_1u_2 + \frac{\partial^2 F_2}{\partial y^2}u_2u_2 \end{pmatrix}_{(E_1^*;\lambda_{SN})} \\ &= \begin{pmatrix} -4x_1^* + 1 + m - \frac{1}{[b+c(\beta-\frac{\lambda_2}{\delta})]^3} \\ 0 \end{pmatrix}. \end{aligned}$$

Finally, we can get

$$V^T F_{\lambda_2}(E_1^*; \lambda_{SN}) = -y_1^* \neq 0,$$

$$V^T[D^2 F(E_1^*; \lambda_{SN})(U, U)] = \frac{2\delta\gamma}{e_{12}}\left[-4x_1^* + 1 + m - \frac{1}{[b + c(\beta - \frac{\lambda_2}{\delta})]^3}\right] \neq 0.$$

Therefore, the model (1.3) can undergo a saddle-node bifurcation when $\lambda_2 = \lambda_{SN} = \beta\delta$. □

5.3. Hopf bifurcation

From Theorem 4.4, E_3^* and E_5^* are always saddle whenever they exist. From Theorem 4.3, E_4^* and E_6^* may be a source or a sink or a center. Therefore, only E_4^* and E_6^* are potentially susceptible to Hopf bifurcation. Given the similarity in properties between E_6^* and E_4^*, we shall focus our discussion on the prototypical internal equilibrium point E_4^*. We designate λ_2 as the variable of interest, which is derived from the condition where the trace equals zero $Tr(J_{E_4^*}) = 0$. As λ_2 varies and surpasses the threshold λ_H, the stability of E_4^* is disrupted. Subsequently, we will furnish a rigorous proof to support this assertion.

Theorem 5.3. *Unstable limit cycles will occur near E_4^* when the first Lyapunov coefficient $l_1 > 0$, and furthermore, the internal equilibrium point E_4^* will also lose its stability due to subcritical Hopf bifurcation when $\lambda_2 = \lambda_H$.*

Proof. We also know $Det(J_{E_4^*}) > 0$ and $Tr(J_{E_4^*}) = 0$ when $\lambda_2 = \lambda_H$. Then,

$$\frac{d}{d\lambda_2} Tr(J_{E_4^*})\bigg|_{\lambda_2=\lambda_H} = \frac{d}{d\lambda_2}\left[-3x_4^{*2} + 2(1+m)x_4^* - (m+\lambda_1) - \frac{y_4^*(1+y_4^*)}{(1+bx_4^*+cy_4^*)^2} + \delta(\beta - \frac{2y_4^*}{x_4^*}) - \lambda_2\right]\bigg|_{\lambda_2=\lambda_H},$$

then

$$\frac{d}{d\lambda_2} Tr(J_{E_4^*})\bigg|_{\lambda_2=\lambda_H} \neq 0.$$

The internal equilibrium point E_4^* will also lose its stability due to subcritical Hopf bifurcation when $\lambda_2 = \lambda_H$.

Furthermore, to assess the stability and direction of the limit cycle formed by this point E_4^*, we need to calculate its first Lyapunov number. This can be achieved by employing a transformation, specifically, $q = x - x_4^*$, $w = y - y_4^*$, we can shift E_4^* to the origin, and gain:

$$\begin{cases} \dot{q} = & a_{10}q + a_{01}w + a_{11}qw + a_{20}q^2 + a_{02}w^2 + a_{30}q^3 \\ & +a_{21}q^2w + a_{12}qw^2 + a_{03}w^3 + M_1(q,w), \\ \dot{w} = & b_{10}q + b_{01}w + b_{11}qw + b_{20}q^2 + b_{02}w^2 + b_{30}q^3 \\ & +b_{21}q^2w + b_{12}qw^2 + b_{03}w^3 + N_1(q,w), \end{cases}$$

where

$$a_{10} = -3x_4^{*2} + 2(1+m)x_4^* - (m+\lambda_1) - \frac{y_4^*(1+cy_4^*)}{(1+bx_4^*+cy_4^*)^2}, \quad a_{01} = -\frac{x_4^*(1+bx_4^*)}{(1+bx_4^*+cy_4^*)^2},$$

$$a_{11} = -\frac{1}{(1+bx_4^*+cy_4^*)^2} - \frac{2bcx_4^*y_4^*}{(1+bx_4^*+cy_4^*)^3}, \quad a_{20} = -3x_4^* + 1 + m + \frac{by_4^*(1+cy_4^*)}{(1+bx_4^*+cy_4^*)^3},$$

$$a_{30} = -1 - \frac{b^2 y_4^*(1+cy_4^*)}{(1+bx_4^*+cy_4^*)^4}, \quad a_{03} = -\frac{c^2 x_4^*(1+bx_4^*)}{(1+bx_4^*+cy_4^*)^4}, \quad a_{02} = \frac{cx_4^*(1+bx_4^*)}{(1+bx_4^*+cy_4^*)^3},$$

$$a_{21} = -\frac{b(cy_4^*-1)}{(1+bx_4^*+cy_4^*)^3} + \frac{3b^2 cx_4^* y_4^*}{(1+bx_4^*+cy_4^*)^4}, \quad a_{12} = -\frac{c(bx_4^*-1)}{(1+bx_4^*+cy_4^*)^3} + \frac{3c^2 bx_4^* y_4^*}{(1+bx_4^*+cy_4^*)^4},$$

$$b_{10} = \frac{\delta y_4^{*2}}{x_4^{*2}}, \quad b_{01} = \delta(\beta - \frac{2y_4^*}{x_4^*}) - \lambda_2, \quad b_{11} = \frac{2\delta y_4^*}{x_4^{*2}}, \quad b_{20} = -\frac{\delta y_4^{*2}}{x_4^{*3}},$$

$$b_{02} = -\frac{\delta}{x_4^*}, \quad b_{30} = \frac{\delta(\beta - \frac{\lambda_2}{\delta})^2}{x_4^{*2}}, \quad b_{21} = \frac{2(\lambda_2 - \delta\beta)}{x_4^{*2}}, \quad b_{12} = \frac{\delta}{x_4^{*2}}, \quad b_{03} = 0,$$

and $M_1(q,w)$, $N_1(q,w)$ are fourth-order infinitesimal quantity.

The first Lyapunov coefficient l_1 is

$$\begin{aligned} l_1 = & \frac{-3\pi}{2a_{01}Det^{\frac{3}{2}}} \Big\{ \Big[a_{10}b_{10}(a_{11}^2 + a_{11}b_{02} + a_{02}b_{11}) + a_{10}a_{01}(b_{11}^2 + a_{20}b_{11} + a_{11}b_{02}) \\ & + b_{10}^2(a_{11}a_{02} + 2a_{02}b_{02}) - 2a_{10}b_{10}(b_{02}^2 - a_{20}a_{02}) \\ & - 2a_{10}a_{01}(a_{20}^2 - b_{20}b_{02}) - a_{01}^2(2a_{20}b_{20} + b_{11}b_{20}) \\ & + (a_{01}b_{10} - 2a_{10}^2)(b_{11}b_{02} - a_{11}a_{20}) \Big] \\ & - (a_{10}^2 + a_{01}b_{10}) \left[3(b_{10}b_{03} - a_{01}a_{30}) + 2a_{10}(a_{21} + b_{12}) + (a_{12}b_{10} - a_{01}b_{21}) \right] \Big\}. \end{aligned}$$

In [49], the dynamic relationship between Lyapunov coefficients and Hopf bifurcation was referred to. The literature indicates that stable limit cycle will emerge near E_4^* when the first Lyapunov coefficient $l_1 < 0$. Additionally, due to supercritical Hopf bifurcation, the internal equilibrium point E_4^* will lose its stability. Unstable limit cycles will occur near E_4^* when the first Lyapunov coefficient $l_1 > 0$, and the internal equilibrium point E_4^* will also lose its stability due to subcritical Hopf bifurcation. □

5.4. Bogdanov-Takens bifurcation

In the previous three sections, we discussed the bifurcation of the codimension-one branch of the model (1.3). Next, we will prove the occurrence of the codimension-two Bogdanov-Takens bifurcation. According to Theorem 4.2, we conclude that E_1^* is a codimension-two cusp when the following conditions meet $\Delta = 0, 1-(m+1)\varphi > 0, (m+\lambda_1)\varphi + \gamma - (m+1) < 0, m = -3x_1^{*2} + (2+2m)x_1^* - \frac{(\beta - \frac{\lambda_2}{\delta})x_1^* + c(\beta - \frac{\lambda_2}{\delta})^2 x_1^{*2}}{(1+bx_1^* + c(\beta - \frac{\lambda_2}{\delta})x_1^*)^2} - \lambda_1 + \lambda_2 - \delta\beta$ and $Det(J_{E_1^*}) \neq 0$. Next, we study the Bogdanov-Takens bifurcation with parameters λ_2 and m.

Theorem 5.4. *If we choose λ_2 and m as bifurcation parameters, then the model (1.3) can generate a Bogdanov-Takens bifurcation around E_1^* with changing parameters (λ_2, m) near (λ_{BT}, m_{BT}) for $\Delta = 0, 1-(m+1)\varphi > 0, (m+\lambda_1)\varphi + \gamma - (m+1) < 0, m = -3x_1^{*2} + (2+2m)x_1^* - \frac{(\beta - \frac{\lambda_2}{\delta})x_1^* + c(\beta - \frac{\lambda_2}{\delta})^2 x_1^{*2}}{(1+bx_1^* + c(\beta - \frac{\lambda_2}{\delta})x_1^*)^2} - \lambda_1 + \lambda_2 - \delta\beta$ and $Det(J_{E_1^*}) \neq 0$, where (λ_{BT}, m_{BT}) denotes the bifurcation threshold value i.e.,*

$$Tr(J_{E_1^*})\,|_{(\lambda_{BT}, m_{BT})} = 0, Det(J_{E_1^*})\,|_{(\lambda_{BT}, m_{BT})} = 0.$$

Proof. To derive precise expressions for saddle points, Hopf, and homoclinic bifurcation curves within a small vicinity around the Bogdanov-Takens point, we convert the model (1.3) into the canonical form of Bogdanov-Takens bifurcation. Subsequently, we introduce a parameter vector (ϵ_1, ϵ_2) that is infinitely close to $(0, 0)$. By applying a minor perturbation, we gradually bring λ_2 and m closer to $\lambda_2 = \lambda_{BT} + \epsilon_1$ and $m = m_{BT} + \epsilon_2$,respectively. Incorporating the perturbation arising from these new parameter variables into the model (1.3), we get

$$\begin{cases} \dot{x} = x(1-x)[x - (m+\epsilon_1)] - \frac{xy}{1+bx+cy} - \lambda_1 x, \\ \dot{y} = \delta y(\beta - \frac{y}{x}) - (\lambda_2 + \epsilon_2)y. \end{cases} \tag{5.1}$$

This can be achieved by employing a transformation, specifically, $\zeta_1 = x - x_1^*$, $\zeta_2 = y - y_1^*$, to shift E_1^* to the origin, and proceeding accordingly:

$$\begin{cases} \frac{d\zeta_1}{dt} = m_{00}(\epsilon) + m_{10}(\epsilon)\zeta_1 + m_{01}(\epsilon)\zeta_2 + m_{20}(\epsilon)\zeta_1^2 + m_{11}(\epsilon)\zeta_1\zeta_2 + m_{02}(\epsilon)\zeta_2^2 + M_1(\zeta_1, \zeta_2, \epsilon), \\ \frac{d\zeta_2}{dt} = n_{00}(\epsilon) + n_{10}(\epsilon)\zeta_1 + n_{01}(\epsilon)\zeta_2 + n_{20}(\epsilon)\zeta_1^2 + n_{11}(\epsilon)\zeta_1\zeta_2 + n_{02}(\epsilon)\zeta_2^2 + N_1(\zeta_1, \zeta_2, \epsilon), \end{cases} \tag{5.2}$$

where

$$m_{00}(\epsilon) = x_1^*(1-x_1^*)[x_1^* - (m+\epsilon_1)] - \frac{x_1^* y_1^*}{1 + bx_1^* + cy_1^*} - \lambda_1 x_1^*,$$

$$m_{10}(\epsilon) = -3{x_1^*}^2 + 2(1 + m + \epsilon_1)x_1^* - (m + \lambda_1 + \epsilon_1) - \frac{y_1^*(1+cy_1^*)}{(1+bx_1^*+cy_1^*)^2},$$

$$m_{01}(\epsilon) = -\frac{x_1^*(1+bx_1^*)}{(1+bx_1^*+cy_1^*)^2}, \quad m_{11}(\epsilon) = -\frac{1 + bx_1^* + cy_1^* + 2bcx_1^* y_1^*}{(1+bx_1^*+cy_1^*)^3},$$

$$m_{20}(\epsilon) = -3x_1^* + 1 + m + \epsilon_1 + \frac{by_1^*(1+cy_1^*)}{(1+bx_1^*+cy_1^*)^3}, \quad m_{02}(\epsilon) = -\frac{cx_1^*(1+bx_1^*)}{(1+bx_1^*+cy_1^*)^3},$$

$$n_{00}(\epsilon) = -\epsilon_2 y_1^*, \qquad n_{10}(\epsilon) = \delta(\beta - \frac{\lambda_2}{\delta})^2, \qquad n_{01}(\epsilon) = \lambda_2 - \delta\beta - \epsilon_2,$$

$$n_{11}(\epsilon) = \frac{2(\beta\delta)}{x_1^*}, \qquad n_{20}(\epsilon) = -\frac{\delta(\beta - \frac{\lambda_2}{\delta})^2}{x_1^*}, \qquad n_{02}(\epsilon) = -\frac{\delta}{x_1^*},$$

and $M_1(\zeta_1, \zeta_2, \varepsilon)$, $N_1(\zeta_1, \zeta_2, \epsilon)$ are third-order infinitesimal quantity.

Then we will perform the transformation

$$X = \zeta_1, \qquad Y = m_{10}(\epsilon)\zeta_1 + m_{01}(\epsilon)\zeta_2,$$

shift the model (5.2) to the model (5.3)

$$\begin{cases} \frac{dX}{dt} = r_{00}(\epsilon) + Y + r_{20}(\epsilon)X^2 + r_{11}(\epsilon)XY + r_{02}(\epsilon)Y^2 + M_1(X, Y, \epsilon), \\ \frac{dY}{dt} = s_{00}(\epsilon) + s_{10}(\epsilon)X + s_{01}(\epsilon)Y + s_{20}(\epsilon)X^2 + s_{11}(\epsilon)XY + s_{02}(\epsilon)Y^2 + N_1(X, Y, \epsilon), \end{cases} \tag{5.3}$$

where

$$r_{00}(\epsilon) = m_{00}(\epsilon), \quad r_{11}(\epsilon) = \frac{m_{01}(\epsilon)m_{11}(\epsilon) - 2m_{02}(\epsilon)m_{10}(\epsilon)}{m_{01}(\epsilon)^2}, \quad r_{02}(\epsilon) = \frac{m_{02}(\epsilon)}{(m_{01}(\epsilon))^2},$$

$$r_{20}(\epsilon) = \frac{m_{01}(\epsilon)^2 m_{20}(\epsilon) - m_{11}(\epsilon)m_{10}(\epsilon)m_{01}(\epsilon) + m_{02}(\epsilon)m_{10}(\epsilon)^2}{m_{01}(\epsilon)^2}, \quad s_{00}(\epsilon) = m_{00}(\epsilon)m_{10}(\epsilon) + n_{00}(\epsilon)m_{01}(\epsilon),$$
$$s_{01}(\epsilon) = m_{10}(\epsilon) + n_{01}(\epsilon), \quad s_{10}(\epsilon) = n_{10}(\epsilon)m_{01}(\epsilon) - n_{01}(\epsilon)m_{10}(\epsilon),$$
$$s_{02}(\epsilon) = \frac{n_{02}(\epsilon)m_{01}(\epsilon) + m_{02}(\epsilon)m_{10}(\epsilon)}{m_{01}(\epsilon)^2},$$
$$s_{11}(\epsilon) = \frac{m_{01}(\epsilon)^2 n_{11}(\epsilon) + m_{11}(\epsilon)m_{10}(\epsilon)m_{01}(\epsilon) - 2m_{01}(\epsilon)m_{10}(\epsilon)n_{02}(\epsilon) - 2m_{02}(\epsilon)m_{10}(\epsilon)^2}{m_{01}(\epsilon)^2},$$
$$s_{20}(\epsilon) = \frac{m_{01}(\epsilon)^3 n_{20}(\epsilon) - m_{01}(\epsilon)m_{10}(\epsilon)^2 m_{11}(\epsilon) + m_{01}(\epsilon)m_{10}(\epsilon)^2 n_{02}(\epsilon) + m_{02}(\epsilon)m_{10}(\epsilon)^3}{m_{01}(\epsilon)^2} + m_{10}(\epsilon)m_{20}(\epsilon)$$
$$- m_{10}(\epsilon)n_{11}(\epsilon),$$

and $M_1(X, Y, \epsilon)$ and $N_1(X, Y, \epsilon)$ are third-order infinitesimal quantity.

So we can add the next change:

$$h_1 = X, \qquad h_2 = r_{00}(\epsilon) + Y + r_{20}(\epsilon)X^2 + r_{11}(\epsilon)XY + r_{02}(\epsilon)Y^2 + N_2(X, Y, \epsilon),$$

shift the model (5.3) to (5.4)

$$\begin{cases} \frac{dh_1}{dt} = h_2, \\ \frac{dh_2}{dt} = f_{00}(\epsilon) + f_{10}(\epsilon)h_1 + f_{01}(\epsilon)h_2 + f_{20}(\epsilon)h_1^2 + f_{11}(\epsilon)h_1h_2 + f_{02}(\epsilon)h_2^2 + N_3(h_1, h_2, \epsilon), \end{cases} \tag{5.4}$$

where

$$\begin{aligned} f_{00}(\epsilon) &= s_{00}(\epsilon) - r_{00}(\epsilon)s_{01}(\epsilon) + r_{00}(\epsilon)^2 s_{02}(\epsilon) - 2r_{00}(\epsilon)r_{02}(\epsilon)s_{00}(\epsilon) + \cdots, \\ f_{10}(\epsilon) &= s_{10}(\epsilon) + r_{11}(\epsilon)s_{00}(\epsilon) - r_{00}(\epsilon)s_{11}(\epsilon) - 2r_{00}(\epsilon)r_{02}(\epsilon)s_{10}(\epsilon) + \cdots, \\ f_{01}(\epsilon) &= s_{01}(\epsilon) + 2r_{02}(\epsilon)s_{00}(\epsilon) - 2r_{00}(\epsilon)s_{02}(\epsilon) - r_{00}(\epsilon)r_{11}(\epsilon) - 4r_{00}(\epsilon)r_{02}(\epsilon)s_{01}(\epsilon) + \cdots, \\ f_{20}(\epsilon) &= s_{20}(\epsilon) - r_{20}(\epsilon)s_{01}(\epsilon) + r_{11}(\epsilon)s_{10}(\epsilon) - 2r_{02}(\epsilon)r_{20}(\epsilon)s_{00}(\epsilon) + 2r_{00}(\epsilon)r_{20}(\epsilon)s_{02}(\epsilon) \\ &\quad - 2r_{00}(\epsilon)r_{02}(\epsilon)s_{20}(\epsilon) + \cdots, \\ f_{11}(\epsilon) &= s_{11}(\epsilon) + 2r_{20}(\epsilon) + 2r_{02}(\epsilon)s_{10}(\epsilon) - 2r_{02}(\epsilon)r_{11}(\epsilon)s_{00}(\epsilon) + 2r_{00}(\epsilon)r_{11}(\epsilon)s_{02}(\epsilon) + \\ &\quad r_{00}(\epsilon)r_{11}(\epsilon)^2 - 4r_{00}(\epsilon)r_{02}(\epsilon)s_{11}(\epsilon) + \cdots, \\ f_{02}(\epsilon) &= s_{02}(\epsilon) + r_{11}(\epsilon) + 2r_{02}(\epsilon)s_{01}(\epsilon) + \cdots, \end{aligned}$$

and $N_3(h_1, h_2, \epsilon)$ is third-order infinitesimal quantity.

Employing a fresh variable τ by $dt = (1 - f_{02}(\epsilon)h_1)d\tau$, then we get

$$\begin{cases} \frac{dh_1}{d\tau} = h_2(1 - f_{02}(\epsilon)h_1), \\ \frac{dh_2}{d\tau} = (1 - f_{02}(\epsilon)h_1)\Big[f_{00}(\epsilon) + f_{10}(\epsilon)h_1 + f_{01}(\epsilon)h_2 + f_{20}(\epsilon)h_1^2 + f_{11}(\epsilon)h_1h_2 + f_{02}(\epsilon)h_2^2 + N_4(h_1, h_2, \epsilon)\Big]. \end{cases} \tag{5.5}$$

Let

$$z_1 = h_1, \quad z_2 = h_2(1 - f_{02}(\epsilon)h_1),$$

then we can shift the model (5.5) to the model (5.6)

$$\begin{cases} \frac{dz_1}{d\tau} = z_2, \\ \frac{dz_2}{d\tau} = k_{00}(\epsilon) + k_{10}(\epsilon)z_1 + k_{01}(\epsilon)z_2 + k_{20}(\epsilon)z_1^2 + k_{11}(\epsilon)z_1z_2 + N_5(z_1, z_2, \epsilon), \end{cases} \tag{5.6}$$

where

$$k_{00}(\epsilon) = f_{00}(\epsilon), \quad k_{01}(\epsilon) = f_{01}(\epsilon), \quad k_{10}(\epsilon) = f_{10}(\epsilon) - 2f_{00}(\epsilon)f_{02}(\epsilon),$$
$$k_{11}(\epsilon) = f_{11}(\epsilon) - f_{01}(\epsilon)f_{02}(\epsilon), \quad k_{20}(\epsilon) = f_{20}(\epsilon) + f_{00}(\epsilon)f_{02}(\epsilon)^2 - 2f_{02}(\epsilon)f_{10}(\epsilon),$$

and $N_4(v_1, v_2, \epsilon)$ is third-order infinitesimal quantity.

We can observe that $h_{20}(\epsilon)$ is an extremely intricate number, rendering it difficult to ascertain the sign of $h_{20}(\epsilon)$ when ϵ_1 and ϵ_2 are small enough. Consequently, to proceed with the subsequent transformation, it is imperative for us to delve into the following two scenarios.

Case 1: For ϵ_1 and ϵ_2 that are small enough, if $k_{20}(\epsilon)$ is greater than 0, we proceed to the next transformation:

$$e_1 = z_1, \quad e_2 = \frac{z_2}{\sqrt{k_{20}(\epsilon)}}, \quad T = \sqrt{k_{20}(\epsilon)}\tau.$$

We can get

$$\begin{cases} \frac{de_1}{dT} = e_2, \\ \frac{de_2}{dT} = R_{00}(\epsilon) + R_{10}(\epsilon)e_1 + R_{01}(\epsilon)e_2 + e_1^2 + R_{11}(\epsilon)e_1e_2 + Q_5(e_1, e_2, \epsilon), \end{cases} \tag{5.7}$$

where

$$R_{00}(\epsilon) = \frac{k_{00}(\epsilon)}{k_{20}(\epsilon)}, \quad R_{10}(\epsilon) = \frac{k_{10}(\epsilon)}{k_{20}(\epsilon)}, \quad R_{01}(\epsilon) = \frac{k_{01}(\epsilon)}{\sqrt{k_{20}(\epsilon)}}, \quad R_{11}(\epsilon) = \frac{k_{11}(\epsilon)}{\sqrt{k_{20}(\epsilon)}},$$

and $Q_5(e_1, e_2, \epsilon)$ is third-order infinitesimal quantity.

Let

$$j_1 = e_1 + \frac{R_{10}(\epsilon)}{2}, \qquad j_2 = e_2,$$

then we have

$$\begin{cases} \frac{dj_1}{dT} = j_2, \\ \frac{dj_2}{dT} = H_{00}(\epsilon) + H_{01}(\epsilon)j_2 + j_1^2 + H_{11}(\epsilon)j_1j_2 + Q_6(j_1, j_2, \epsilon), \end{cases} \tag{5.8}$$

where

$$H_{00}(\epsilon) = R_{00}(\epsilon) - \frac{1}{4}R_{10}^2(\epsilon), \quad H_{01}(\epsilon) = R_{01}(\epsilon) - \frac{1}{2}R_{10}(\epsilon)R_{11}(\epsilon), \quad H_{11}(\epsilon) = R_{11}(\epsilon),$$

and $Q_6(j_1, j_2, \epsilon)$ is third-order infinitesimal quantity.

In case of $k_{11}(\epsilon) \neq 0$, then we have $H_{11}(\epsilon) = R_{11}(\epsilon) = \frac{k_{11}(\epsilon)}{\sqrt{k_{20}(\epsilon)}} \neq 0$, and give the next transformation:

$$X = H_{11}^2(\epsilon)j_1, \qquad Y = H_{11}^3(\epsilon)j_2, \qquad t = \frac{1}{H_{11}(\epsilon)}T,$$

then we have

$$\begin{cases} \frac{dX}{dt} = Y, \\ \frac{dY}{dt} = \xi_1(\epsilon) + \xi_2(\epsilon)Y + X^2 + XY + Q_7(X, Y, \epsilon), \end{cases} \tag{5.9}$$

where

$$\xi_1(\epsilon) = H_{00}(\epsilon)H_{11}(\epsilon)^4, \quad \xi_2(\epsilon) = H_{01}(\epsilon)H_{11}(\epsilon),$$

and $Q_7(X, Y, \epsilon)$ is third-order infinitesimal quantity.

Case 2: For ϵ_1 and ϵ_2 that are small enough, if $k_{20}(\epsilon)$ is smaller than 0, we proceed to the next transformation:

$$e_1' = z_1, \quad e_2' = \frac{z_2}{\sqrt{-k_{20}(\epsilon)}}, \quad T' = \sqrt{-k_{20}(\epsilon)}\tau.$$

We can get

$$\begin{cases} \frac{de_1'}{dT'} = e_2', \\ \frac{de_2'}{dT'} = R_{00}'(\epsilon) + R_{10}'(\epsilon)e_1' + R_{01}'(\epsilon)e_2' + {e_1'}^2 + R_{11}'(\epsilon)e_1'e_2' + Q_5'(e_1', e_2', \epsilon), \end{cases} \tag{5.10}$$

where

$$R_{00}'(\epsilon) = -\frac{k_{00}(\epsilon)}{k_{20}(\epsilon)}, \quad R_{10}'(\epsilon) = -\frac{k_{10}(\epsilon)}{k_{20}(\epsilon)}, \quad R_{01}'(\epsilon) = \frac{k_{01}(\epsilon)}{\sqrt{-k_{20}(\epsilon)}}, \quad R_{11}'(\epsilon) = \frac{k_{11}(\epsilon)}{\sqrt{-k_{20}(\epsilon)}},$$

and $Q_5'(e_1', e_2', \epsilon)$ is third-order infinitesimal quantity.

Let

$$j_1' = e_1' - \frac{R_{10}'(\epsilon)}{2}, \qquad j_2' = e_2',$$

we have

$$\begin{cases} \frac{dj_1'}{dT'} = j_2', \\ \frac{dj_2'}{dT'} = H_{00}'(\epsilon) + H_{01}'(\epsilon)j_2' + {j_1'}^2 + H_{11}'(\epsilon)j_1'j_2' + Q_6'(j_1', j_2', \epsilon), \end{cases} \tag{5.11}$$

where

$$H_{00}'(\epsilon) = R_{00}'(\epsilon) - \frac{1}{4}R_{10}'(\epsilon)^2, \quad H_{01}'(\epsilon) = R_{01}'(\epsilon) - \frac{1}{2}R_{10}'(\epsilon)R_{11}'(\epsilon), \quad H_{11}'(\epsilon) = R_{11}'(\epsilon),$$

and $Q_6(j_1', j_2', \epsilon)$ is third-order infinitesimal quantity.

In case of $k_{11}(\epsilon) \neq 0$, then we have $H_{11}'(\epsilon) = R_{11}'(\epsilon) = \frac{k_{11}(\epsilon)}{\sqrt{-k_{20}(\epsilon)}} \neq 0$, and go on the next transformation:

$$X' = H_{11}'(\epsilon)^2 j_1', \qquad Y' = H_{11}'(\epsilon)^2 j_2', \qquad t' = \frac{1}{H_{11}'(\epsilon)}T',$$

we have

$$\begin{cases} \frac{dX'}{dt'} = Y', \\ \frac{dY'}{dt'} = \xi_1'(\epsilon) + \xi_2'(\epsilon)Y' + X'^2 + X'Y' + Q_7'(X', Y', \epsilon), \end{cases} \tag{5.12}$$

where

$$\xi_1'(\epsilon) = H_{00}'(\epsilon)H_{11}'(\epsilon)^4, \quad \xi_2'(\epsilon) = H_{01}'(\epsilon)H_{11}'(\epsilon),$$

and $Q_7'(X', Y', \epsilon)$ is third-order infinitesimal quantity.

To reduce the number of cases to be taken into account, we will retain $\xi_1(\epsilon)$ and $\xi_2(\epsilon)$ to stand for $\xi_1'(\epsilon)$ and $\xi_2'(\epsilon)$ in (5.12). When the matrix $\left|\frac{\partial(\xi_1,\xi_2)}{\partial(\epsilon_1,\epsilon_2)}\right|$ is nonsingular, then the transformation is a homeomorphism in a adequately small domain of the $(0, 0)$. Moreover, based on the above conditions, it is evident that ξ_1, ξ_2 are two independent variables. From the conclusions in [49], it is obvious that B-T bifurcation is formed when $\epsilon = (\epsilon_1, \epsilon_2)$ is in a fully small domain of the (0,0). Accordingly, the local formulas near the

origin of bifurcation curves can be written as ("+" expresses $k_{20}(\epsilon) > 0$ and "-" expresses $k_{20}(\epsilon) < 0$):
1) The saddle-node bifurcation curve can be written as
$SN = \{(\epsilon_1, \epsilon_2) : \xi_1(\epsilon_1, \epsilon_2) = 0, \xi_2(\epsilon_1, \epsilon_2) \neq 0\}$.
2) The Hopf bifurcation curve can be written as
$H = \left\{(\epsilon_1, \epsilon_2) : \xi_2(\epsilon_1, \epsilon_2) = \pm\sqrt{-\xi_1(\epsilon_1, \epsilon_2)}, \xi_1(\epsilon_1, \epsilon_2) < 0\right\}$.
3) The homoclinic bifurcation curve can be written as
$HL = \left\{(\epsilon_1, \epsilon_2) : \xi_2(\epsilon_1, \epsilon_2) = \pm\frac{5}{7}\sqrt{-\xi_1(\epsilon_1, \epsilon_2)}, \xi_1(\epsilon_1, \epsilon_2) < 0\right\}$. □

Based on mathematical theory derivation, we obtained threshold conditions for inducing transcritical bifurcation, saddle-node bifurcation, Hopf bifurcation, and Bogdanov-Takens bifurcation in the model (1.3). These conditions can serve as the theoretical basis for subsequent numerical simulations, and directly indicate that the values of some key parameters can seriously affect the bifurcation dynamics evolution process of the model (1.3). Moreover, according to the theoretical derivation process, it is worth emphasizing that the size of the predator and prey harvesting behavior can alter the intrinsic dynamic characteristics of the model (1.3).

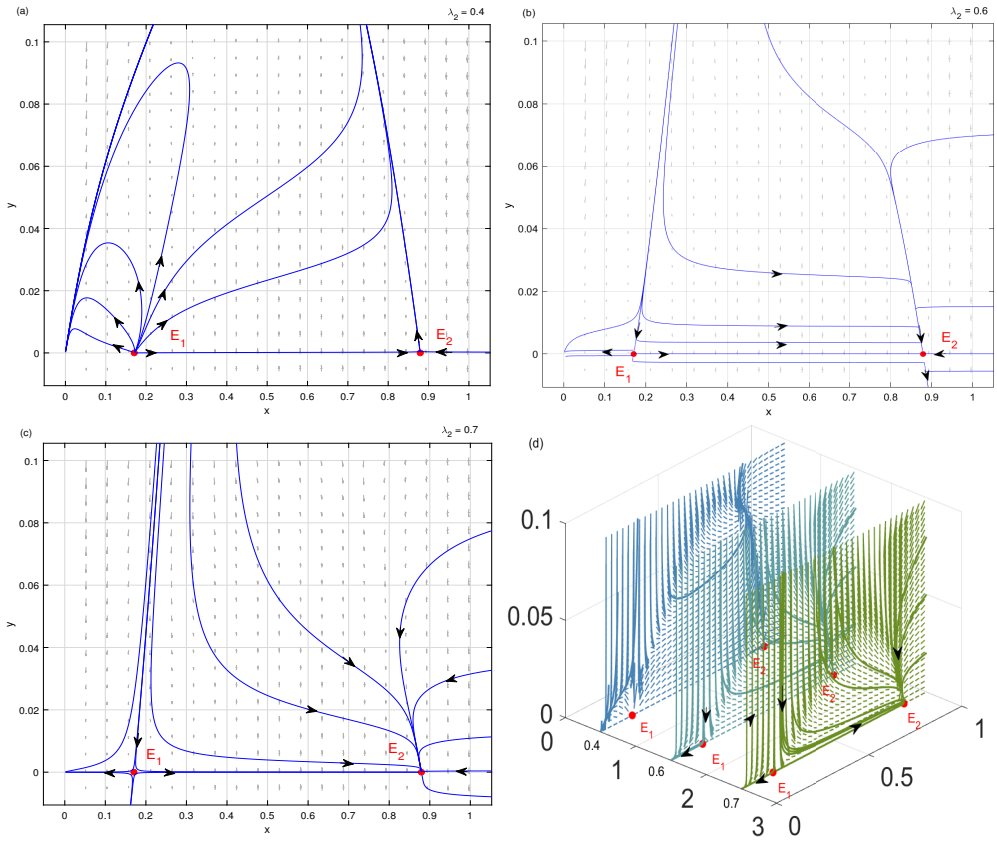

Figure 1. A transcritical bifurcation occurs based on the change of λ_2. (a)–(c) show the stability of boundary equilibrium point E_1 and E_2: (a) unstable node E_1 and unstable saddle E_2; (b) non attracting saddle-node E_1 and attracting saddle-node E_2; (c) unstable saddle E_1 and globally asymptotically stable node E_2; (d) A locally enlarged view of the entire transcritical bifurcation process.

6. Simulation analysis and results

To verify the effectiveness of theoretical derivation and explore the bifurcation dynamics evolution process of the model (1.3), we conduct relevant bifurcation dynamics numerical simulations on the model (1.3).

According to Theorem 5.1, we can choose $m = 0.05, b = 0.2, c = 0.2, \beta = 2, s = 0.3, \lambda_1 = 0.1$, and we can directly calculate $\lambda_{TC} = 0.6$; thus, we can numerically simulate the dynamic evolution process of the model (1.3) undergoing transcritical bifurcation, and the detailed results can be seen in Figure 1. When the value of λ_2 is 0.4, the model (1.3) has two boundary equilibrium points E_1 and E_2, the boundary equilibrium point E_1 is an unstable node and the boundary equilibrium point E_2 is a saddle (see Figure 1(a)). When the value of λ_2 is equal to 0.6, the boundary equilibrium points E_1 and E_2 are saddle-node (see Figure 1(b)). When the value of λ_2 is greater to 0.6, the model (1.3) has a saddle E_1 and a stable node E_2 (see Figure 1(c)). Therefore, this numerical simulation result not only points out the feasibility of Theorem 5.1, but also indicates that excessive harvesting of predator can lead to the extinction of predator population.

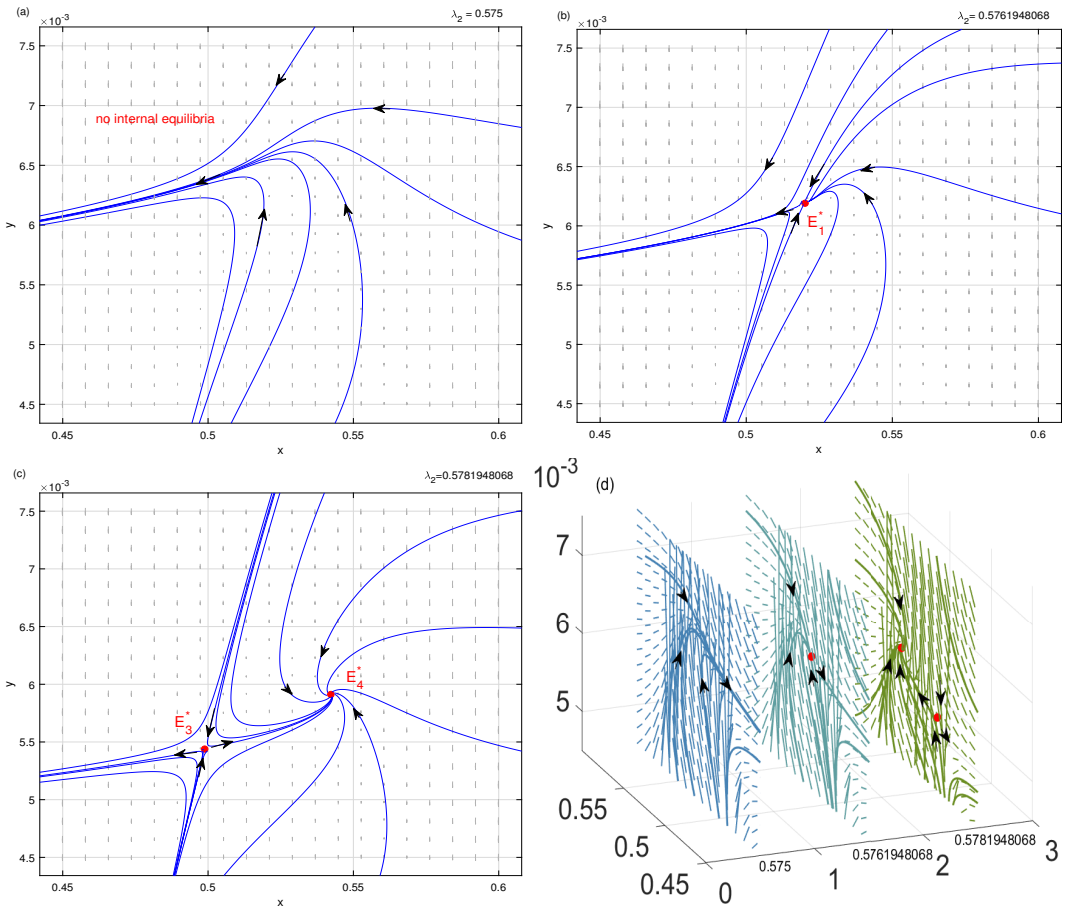

Figure 2. A saddle-node bifurcation occurs based on the change of λ_2.(a) the model (1.3) has no internal equilibria when the value of λ_2 is smaller than 0.5761948068; (b) unique equilibrium point E_1^*, which is a saddle-node; (c) two internal equilibria E_3^* and E_4^*, a saddle and a node; (d)a locally enlarged view of the entire saddle-node bifurcation process.

Based on the condition of Theorem 5.2, we can take $m = 0.05, b = 0.2, c = 0.2, \beta = 0.3, \delta = 2, \lambda_1 = 0.22$ thus, we obtain $\lambda_{SN} = 0.5761948068$, which means that the model (1.3) will experience a saddle-node bifurcation as λ_2 varies around λ_{SN}. Furthermore, it is worth noting from Figure 2 that the model (1.3) has no internal equilibrium point when $\lambda_2 = 0.575$, has an internal equilibrium point E_1^* when $\lambda_2 = 0.5761948068$, and has two internal equilibrium points E_3^* and E_4^* when $\lambda_2 = 0.5781948068$. Furthermore, it is worth emphasizing that the internal equilibrium point E_3^* is a saddle and the internal equilibrium point E_4^* is a stable node. Hence, it not only proves that Theorem 5.2 is valid, but also infers that prey and predator can form a constant steady state persistent survival mode, which implies that harvesting predator reasonably can be beneficial for the sustainable survival of prey and predator.

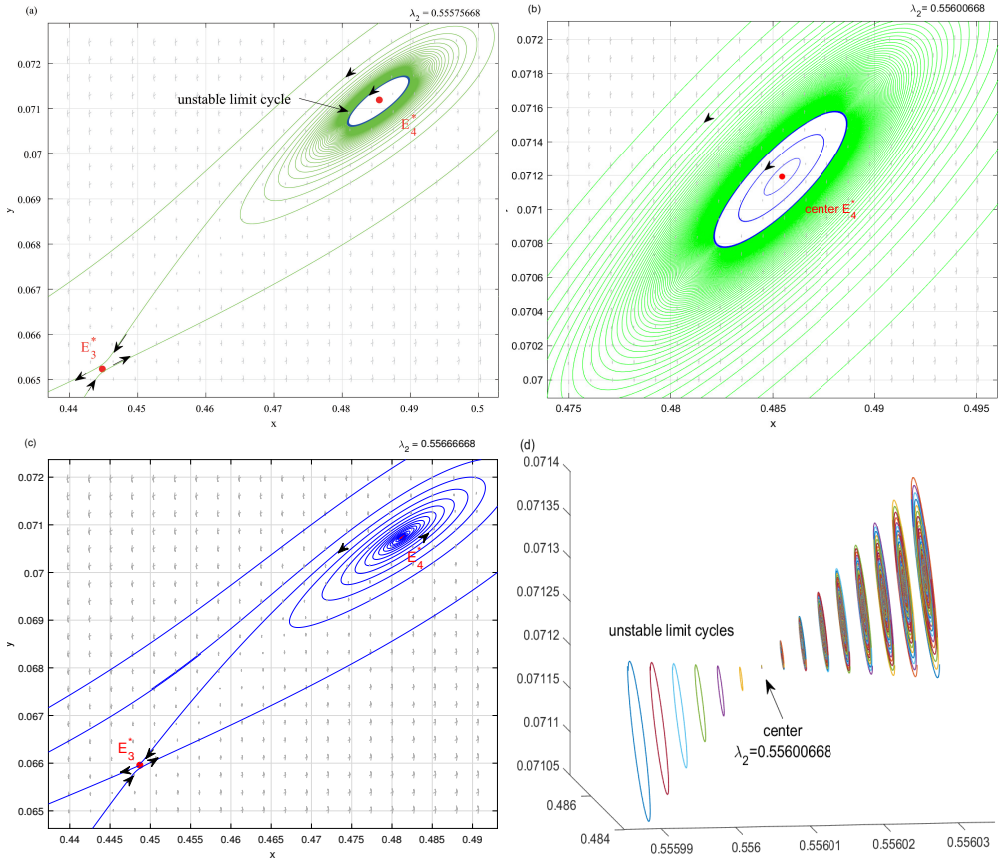

Figure 3. A Hopf bifurcation occurs based on the change of λ_2. (a) an unstable focus E_4^*; (b) unstable limit cycles around the center E_4^*; (c)a stable focus E_4^*; (d) the Hopf bifurcation diagram represents the center E_4^* and unstable limit cycles with different λ_2 values.

Based on Theorem 5.3, we take $m = 0.05, b = 0.2, c = 0.2, \beta = 2, \delta = 0.3, \lambda_1 = 0.16$, then we can obtain $\lambda_H = 0.55600668$. It is obvious to find from Figure 3 that the model (1.3) has an unstable limit cycle when $\lambda_2 = 0.55575668 < 0.55600668$. This is because the corresponding first Lyapunov number $l_1 = 669.843133\pi > 0$, which indicates that the limit cycle is unstable, then the unstable focus E_4^* transforms into the center when $\lambda_2 = 0.55600668$, and the internal equilibrium point E_4^* turns into a stable focus from the center when $\lambda_2 = 0.556666668 > 0.55600668$. Furthermore, it is worth pointing out from Figure 3(d) that the model (1.3) visually displays a Hopf bifurcation process as the parameter λ_2 value increases, and if the parameter λ_2 value increases, the amplitude of the limit cycle will also

increase. Therefore, it is necessary to clarify that the model (1.3) has undergone a subcritical Hopf bifurcation, which can induce the formation of periodic oscillation persistent survival mode between prey and predator.

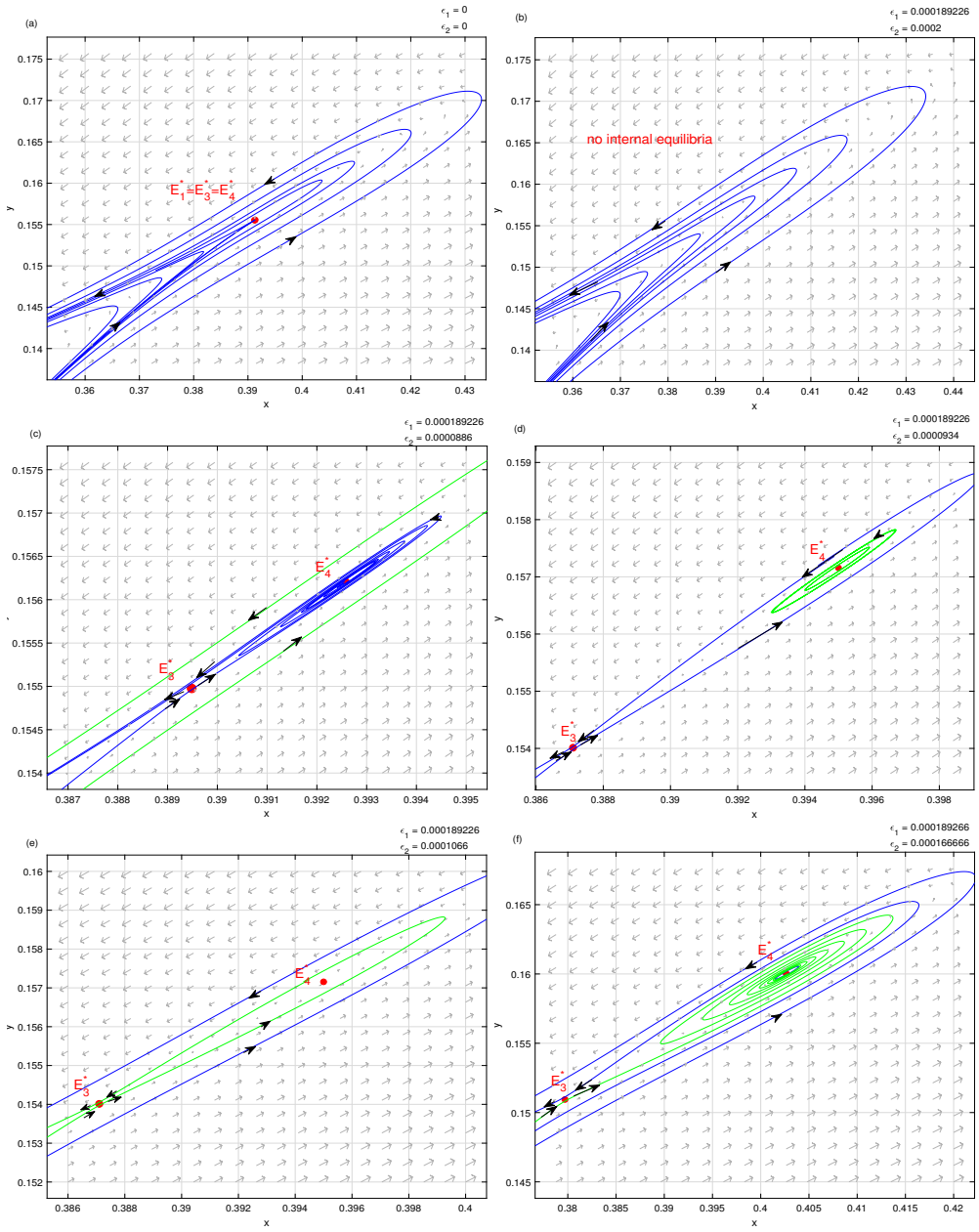

Figure 4. The dynamic evolution process of B-T bifurcation of the model (5.1). (a) A cusp with codimension 2 when $(\epsilon_1, \epsilon_2) = (0, 0)$; (b) no equilibrium point when $(\epsilon_1, \epsilon_2) = (0.000189226; 0.0002)$; (c) unstable saddle and an unstable focus when $(\epsilon_1, \epsilon_2) = (0.000189226; 0.0000886)$; (d) unstable limit cycles revolve around a center and a saddle when $(\epsilon_1, \epsilon_2) = (0.000189226; 0.0000934)$; (e) a stable focus surrounded by an unstable homoclinic orbit and a saddle when $(\epsilon_1, \epsilon_2) = (0.000189226; 0.0001066)$; and (f) a saddle and a stable focus when $(\epsilon_1, \epsilon_2) = (0.000189226; 0.000166666)$.

Based on Theorem 5.4, we take $m = 0.050810774, b = 0.2, c = 0.2, \beta = 2, \delta = 0.3, \lambda_1 = 0.16$; hence, we can deduce $m_{BT} = 0.050810774$ and $\lambda_{BT} = 0.5562939$, and conduct relevant numerical simulations on Bogdanov-Takens bifurcation, the detailed numerical simulation results are shown in Figure 4. It is must be worth emphasizing from Figure 4 that if there are slight changes in the values of key parameters m and λ_2 near the key values $m_{BT} = 0.050810774$ and $\lambda_{BT} = 0.5562939$, the dynamic behavior of the model (5.1) will undergo fundamental changes, which contains that the persistent survival model of prey and predators have undergone dynamic changes. Therefore, it is easy to see from Figure 4 that the persistent survival mode of prey and predator may exhibit constant steady state or periodic oscillation under the disturbance of key parameter m and λ_2 values, which also directly indicates that the value of key parameters m and λ_2 can synergistically affect the persistent survival mode of prey and predator.

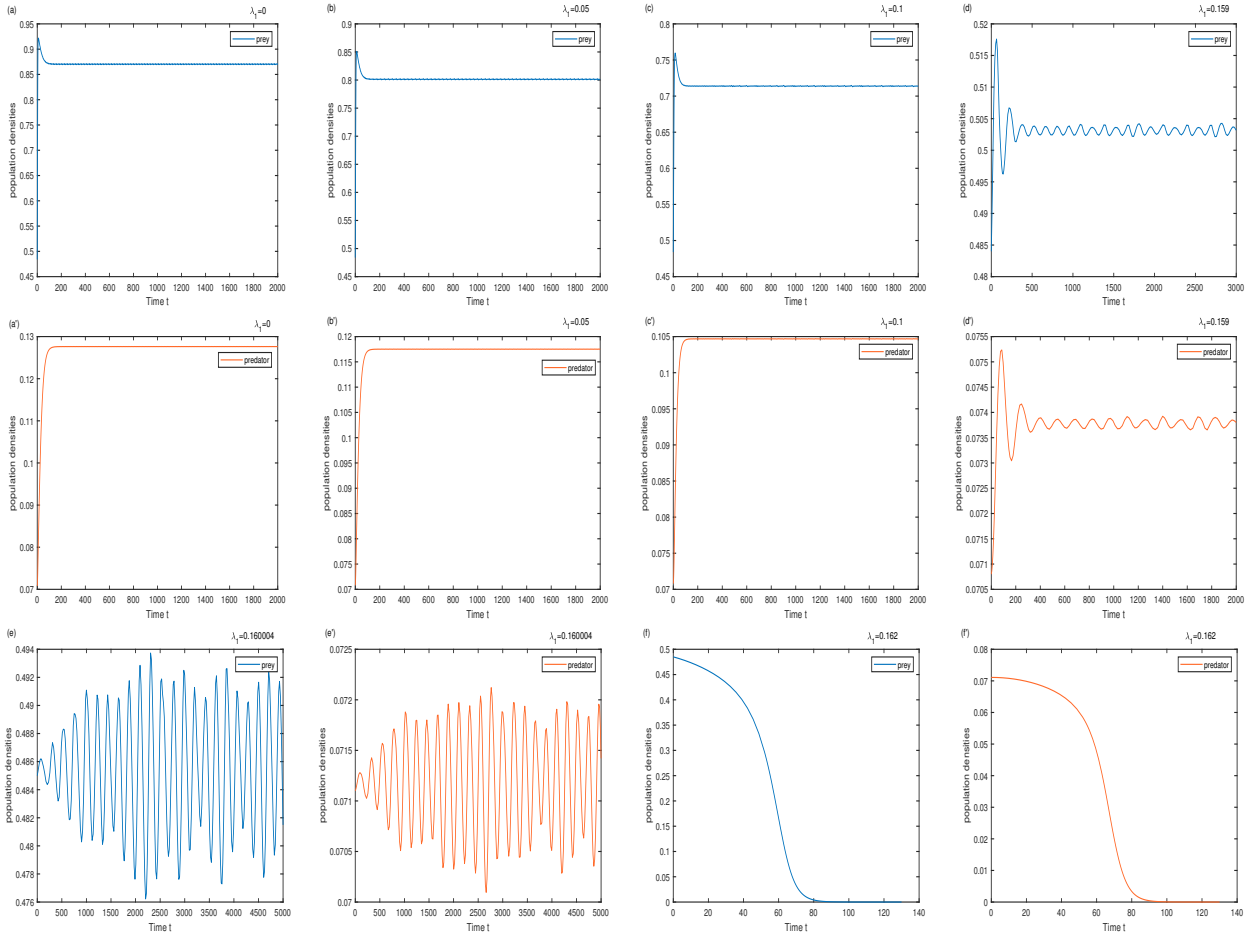

Figure 5. (a)–(f') The time series chart of prey and predator with different parameter λ_1 values.

To explore how the harvesting effort of prey affects the dynamic behavior of the model (1.3) and persistent survival mode between prey and predator, we will select parameter λ_1 as a control parameter to simulate the relevant dynamic behavior, the detailed simulation results are shown in Figure 5. It is obvious to know that the model (1.3) has a stable internal equilibrium point when λ_1 is $0, 0.05$ and 0.1 respectively, which means that prey and predator can coexist in a constant steady state. Furthermore, it is worth pointing out that the model (1.3) has a limit cycle when λ_1 is 0.15, which means that prey

and predator can coexist in periodic oscillation. Moreover, it is easy to see that the model (1.3) has a chaotic attractor when λ_1 is 0.160004, which means that prey and predator can coexist in an irregular state. However, it must also be emphasized that prey and predator will gradually become extinct when λ_1 is 0.162. Therefore, it is worth summarizing that prey and predator are prone to persistent survival when the parameter λ_1 values are relatively small, that si to say, if we want to maintain the sustainable survival of predatory ecosystems, we cannot over capture prey population.

The above numerical simulation results not only verify the feasibility and effectiveness of the theoretical derivation, but also dynamically display the specific dynamic evolution process of the model (1.3), and intuitively demonstrate the persistent survival mode of prey and predator, especially constant steady state mode and periodic oscillation mode, which are particularly beneficial for the long-term and sustainable cyclic development of predatory ecosystems.

7. Conclusions

As is well known, the Allee effect and harvesting effort can seriously affect the dynamic behaviors of predator-prey model. Thus, we introduce the Allee effect and harvesting effort to construct a predator-prey model, the main purpose is to explore how they affect the bifurcation dynamics evolution process of the model (1.3), and reveal the persistent survival mode of prey and predator and its driving mechanisms. Mathematical theoretical work mainly investigate the existence and stability of some equilibrium points, as well as the triggering conditions of specific bifurcation dynamics, such as transcritical bifurcation, saddle-node bifurcation, Hopf bifurcation, and Bogdanov-Takens bifurcation, which can provide a theoretical basis for elucidating the driving mechanisms behind the formation of specific persistent survival mode between prey and predator. The numerical simulation work show the evolution process of the specific bifurcation dynamics behavior of the model (1.3), which can visualize the persistent survival mode and the dynamic variation characteristics of population density.

Based on mathematical theory and numerical simulation results, it is worth emphasizing that Allee effect and harvesting effort seriously affect the dynamic behavior of the model (1.3), especially bifurcation dynamics. Furthermore, it must be pointed out that the magnitude of harvesting efforts on predator can trigger the formation of transcritical bifurcation, saddle-node bifurcation and Hopf bifurcation. The saddle-node bifurcation can cause the model (1.3) to generate a stable internal equilibrium point, which can lead to the formation of a constant steady state persistent survival mode between prey and predator. The Hopf bifurcation can induce the occurrence of periodic solution in the model (1.3), which can result in the formation of a periodic oscillation persistent survival mode between prey and predator. Therefore, it is an important discovery that the saddle-node bifurcation and Hopf bifurcation are intrinsic driving force behind the formation of specific persistent survival mode between prey and predator. Moreover, it is worth clarifying that Allee effect in prey and harvesting effort in predator are able to collaboratively drive the model (1.3) through Bogdanov-Takens bifurcation, which implies that prey and predator can switch back and forth between constant steady state persistent survival mode and periodic oscillation persistent survival mode under small perturbations in key parameter values. Furthermore, it is necessary to emphasize that appropriate harvesting effort on the prey population can also enable prey and predator to coexist persistently in constant steady state, periodic oscillation, and irregularity state.

One innovation of this research is the introduction of harvesting effort for prey and predator in the

ecological modeling process, which not only makes the ecological model (1.3) more controllable, but also enhances its applicability. Another innovation of this research is to reveal the persistent survival mode and underlying driving mechanism from the perspective of bifurcation dynamics evolution, which directly elucidates the impact mechanism of Allee effect and harvesting effort on the bifurcation dynamics of ecological model (1.3). Furthermore, it is worth comparing and explaining that the introduction of harvesting effort in the original model can form a periodic oscillation persistent survival mode between predator and prey, which directly indicates that regulatory measures can prevent the outbreak of algal bloom. Furthermore, it is worth noting that the introduction of Allee effect in the original model can synergistically enrich the dynamic behavior with other key parameters.

Although we obtained some theoretical and numerical results, there is much work to be studied, such as the spatial interaction characteristics between prey and predator, the prey substitutability in predator population, and the controllability problem based on state feedback. However, it is hoped that the research findings of this paper can contribute to the rapid development of predator-prey model dynamics research.

Use of AI tools declaration

The authors declare they have not used Artificial Intelligence (AI) tools in the creation of this article.

Acknowledgments

This work was supported by the National Natural Science Foundation of China (Grants N0.31570364 and No.61871293), the Zhejiang Province College Student Science and Technology Innovation Activity Plan (New Talent Plan) (No.2024R429A010), and the National Key Research and Development Program of China (Grant No.2018YFE0103700).

Conflict of interest

The authors declare there is no conflicts of interest.

References

1. G. B. Gao, D. Bai, T. L. Li, J. Li, Y. Jia, J. Li, et al., Understanding filamentous cyanobacteria and their adaptive niches in Lake Honghu, a shallow eutrophic lake, *J. Environ. Sci.*, **152** (2025), 219–234. https://doi.org/10.1016/j.jes.2024.05.010.
2. H. Fang, T. Wu, S. T. Ma, Y. Miao, X. Wang, Biogenic emission as a potential source of atmospheric aromatic hydrocarbons: Insights from a cyanobacterial bloom-occurring eutrophic lake, *J. Environ. Sci.*, **151** (2025), 497–504. https://doi.org/10.1016/j.jes.2024.04.011.
3. X. X. Liu, Y. J. Lou, Global dynamics of a predator–prey model, *J. Math. Anal. Appl.*, **371** (2010), 323–340. https://doi.org/10.1016/j.jmaa.2010.05.037.
4. A. J. Lotka, Elements of physical biology, *Nature*, **461** (1925). https://doi.org/10.1038/116461b0
5. V. Volterra, Fluctuations in the abundance of a species considered mathematically, *Nature*, **1926** (1926), 558–560. https://doi.org/10.1038/118558a0

6. Y. Yao, L. L. Liu, Dynamics of a predator–prey system with foraging facilitation and group defense, *Commun. Nonlinear Sci. Numer. Simul.*, **138** (2024), 108198. https://doi.org/10.1016/j.cnsns.2024.108198.
7. A. A. Thirthar, P. Panja, S. J. Majeed, K. S. Nisar, Dynamic interactions in a two-species model of the mammalian predator–prey system: The influence of Allee effects, prey refuge, water resources, and moonlights, *Partial Differ. Equations Appl. Math.*, **11** (2024), 100865. https://doi.org/10.1016/j.padiff.2024.100865.
8. Y. J. Li, M. X. He, Z. Li, Dynamics of a ratio-dependent Leslie–Gower predator–prey model with Allee effect and fear effect, *Math. Comput. Simul.*, **201** (2022), 417–439. https://doi.org/10.1016/j.matcom.2022.05.017.
9. X. Chen, W. Yang, Impact of fear-induced group defense in a Monod–Haldane type prey–predator model, *J. Appl. Math. Comput.*, **212** (2024), 3331–3368. https://doi.org/10.1007/s12190-024-02101-8
10. D. Das, T. K. Kar, D. Pal, The impact of invasive species on some ecological services in a harvested predator–prey system, *Math. Comput. Simul.*, **212** (2023), 66–90. https://doi.org/10.1016/j.matcom.2023.04.024.
11. T. K. Ang, H. M. Safuan, Dynamical behaviors and optimal harvesting of an intraguild prey-predator fishery model with Michaelis-Menten type predator harvesting, *BioSystems*, **202** (2021), 104357. https://doi.org/10.1016/j.biosystems.2021.104357.
12. L. N. Guin, H. Baek, Bistability in modified Holling II response model with harvesting and Allee effect: Exploring transitions in a noisy environment, *Math. Comput. Simul.*, **146** (2018), 100–117. https://doi.org/10.1016/j.matcom.2017.10.015.
13. L. N. Guin, S. Djilali, S. Chakravarty, Bistability Cross-diffusion-driven instability in an interacting species model with prey refuge, *Chaos, Solitons Fractals*, **153** (2021), 111501. https://doi.org/10.1016/j.chaos.2021.111501.
14. P. H. Leslie, Some further notes on the use of matrices in population mathematics, *Biometrika*, **35** (1948), 213–245. https://doi.org/10.2307/2332342
15. P. H. Leslie, A stochastic model for studying the properties of certain biological systems by numerical methods, *Biometrika*, **45** (1958), 16–31. https://doi.org/10.1093/biomet/45.1-2.16
16. A. Korobeinikov, A Lyapunov function for Leslie-Gower predator-prey models, *Appl. Math. Lett.*, **14** (2001), 697–699. https://doi.org/10.1016/S0893-9659(01)80029-X.
17. X. B. Zhang, Q. An, L. Wang, Spatiotemporal dynamics of a delayed diffusive ratio-dependent predator-prey model with fear effect, *Nonlinear Dyn.*, **105** (2021), 3775–3790. https://doi.org/10.1007/s11071-021-06780-x
18. P. P. Cong, M. Fan, X. F. Zou, Dynamics of a three-species food chain model with fear effect, *Commun. Nonlinear Sci. Numer. Simul.*, **99** (2021), 105809. https://doi.org/10.1016/j.cnsns.2021.105809
19. Q. Li, Y. Y. Zhang, Y. N. Xiao, Canard phenomena for a slow-fast predator-prey system with group defense of the prey, *J. Math. Anal. Appl.*, **527** (2023), 127418. https://doi.org/10.1016/j.jmaa.2023.127418
20. D. Mukherjee, C. Maji, Bifurcation analysis of a Holling type II predator-prey model with refuge, *Chin. J. Phys.*, **65** (2020), 153–162. https://doi.org/10.1016/j.cjph.2020.02.012

21. K. Chakraborty, S. S. Das, Biological conservation of a prey-predator system incorporating constant prey refuge through provision of alternative food to predators: a theoretical study, *Acta Biotheor.*, **62** (2014), 183–205. https://doi.org/10.1007/s10441-014-9217-9.

22. D. Sen, S. Ghorai, S. Sharma, M. Banerjee, Allee effect in prey's growth reduces the dynamical complexity in prey-predator model with generalist predator, *Appl. Math. Modell.*, **91** (2021), 768–790. https://doi.org/10.1016/j.apm.2020.09.046

23. D. Y. Bai, Y. Kang, S. G. Ruan, L. Wang, Dynamics of an intraguild predation food web model with strong Allee effect in the basal prey, *Nonlinear Anal. Real World Appl.*, **58** (2021), 103206. https://doi.org/10.1016/j.nonrwa.2020.103206

24. V. Tiwari, J. P. Tripathi, R. K. Upadhyay, Y. P. Wu, J. S. Wang, G. Q. Sun, Predator-prey interaction system with mutually interfering predator: role of feedback control, *Appl. Math. Modell.*, **87** (2022), 222–244. https://doi.org/10.1016/j.apm.2020.04.024

25. P. P. Cong, M. Fan, X. F. Zou, Dynamics of a three-species food chain model with fear effect, *Commun. Nonlinear Sci. Numer. Simul.*, **99** (2021), 105809. https://doi.org/10.1016/j.cnsns.2021.105809

26. X. X. Li, H. G. Yu, C. J. Dai, Z. Ma, Q. Wang, M. Zhao, Bifurcation analysis of a new aquatic ecological model with aggregation effect, *Math. Comput. Simul.*, **190** (2021), 75–96. https://doi.org/10.1016/j.matcom.2021.05.015

27. W. C. Allee, *Animal Aggregations, A Study in General Sociology*, The University of Chicago Press, **1431** (1931). https://doi.org/10.5962/bhl.title.7313

28. C. Arancibia–Ibarra, J. Flores, Dynamics of a Leslie–Gower predator–prey model with Holling type II functional response, Allee effect and a generalist predator, *Math. Comput. Simul.*, **188** (2021), 1–22. https://doi.org/10.1016/j.matcom.2021.03.035

29. M. X. He, Z. Li, Global dynamics of a Leslie–Gower predator–prey model with square root response function, *Appl. Math. Lett.*, **140** (2023), 108561. https://doi.org/10.1016/j.aml.2022.108561

30. A. Ali, S. Jawad, A. H. Ali, M. Winter, Stability analysis for the phytoplankton-zooplankton model with depletion of dissolved oxygen and strong Allee effects, *Results Eng.*, **22** (2024), 102190. https://doi.org/10.1016/j.rineng.2024.102190

31. S. Akhtar, N. H. Gazi, S. Sarwardi, Mathematical modelling and bifurcation analysis of an eco-epidemiological system with multiple functional responses subjected to Allee effect and competition, *Results Control Optim.*, **15** (2024), 100421. https://doi.org/10.1016/j.rico.2024.100421

32. A. Alamin, A. Akgül, M. Rahaman, S. P. Mondal, S. Alam, Dynamical behaviour of discrete logistic equation with Allee effect in an uncertain environment, *Results Control Optim.*, **12** (2023), 100254. https://doi.org/10.1016/j.rico.2023.100254

33. S. B. Hsu, T. W. Huang, Global stability for a class of predator-prey systems, *SIAM J. Appl. Math*, **55** (1995), 763–783. https://doi.org/10.1137/S0036139993253201

34. S. J. Lv, Z. M. Fang, The dynamic complexity of a host–parasitoid model with a Beddington-DeAngelis functional response, *Chaos, Solitons Fractals*, **41** (2009), 2617–2623. https://doi.org/10.1016/j.chaos.2008.09.052

35. M. Zhao, S. J. Lv, Chaos in a three-species food chain model with a Beddington-DeAngelis functional response, *Chaos, Solitons Fractals*, **40** (2009), 2305–2316. https://doi.org/10.1016/j.chaos.2007.10.025

36. S. W. Zhang, L. S. Chen, A study of predator–prey models with the Beddington–DeAnglis functional response and impulsive effect, *Chaos, Solitons Fractals*, **27** (2006), 237–248. https://doi.org/10.1016/j.chaos.2005.03.039

37. S. Creel, D. Christianson, Relationships between direct predation and risk effects, *Trends Ecol. Evol.*, **23** (2008), 194–201. https://doi.org/10.1016/j.tree.2007.12.004

38. A. K. Umrao, S. Roy, P. K. Tiwari, P. K. Srivastava, Dynamical behaviors of autonomous and nonautonomous models of generalist predator–prey system with fear, mutual interference and nonlinear harvesting, *Chaos, Solitons Fractals*, **183** (2024), 114891. https://doi.org/10.1016/j.chaos.2024.114891

39. Y. C. Xu, Y. Yang, F. W. Meng, S. Ruan, Degenerate codimension-2 cusp of limit cycles in a Holling–Tanner model with harvesting and anti-predator behavior, *Nonlinear Anal. Real World Appl.*, **76** (2024), 103995. https://doi.org/10.1016/j.nonrwa.2023.103995

40. S. Mandal, N. Sk, P. K. Tiwari, J. Chattopadhyay, Bistability in modified Holling II response model with harvesting and Allee effect: Exploring transitions in a noisy environment, *Chaos, Solitons Fractals*, **178** (2024), 114365. https://doi.org/10.1016/j.chaos.2023.114365

41. X. B. Zhang, H. L. Zhu, Q. An, Dynamics analysis of a diffusive predator-prey model with spatial memory and nonlocal fear effect, *J. Math. Anal. Appl.*, **525** (2023), 127123. https://doi.org/10.1016/j.jmaa.2023.127123

42. W. J. Li, G. D. Li, J. D. Cao, F. Xu, Dynamics analysis of a diffusive SIRI epidemic system under logistic source and general incidence rate, *Commun. Nonlinear Sci. Numer. Simul.*, **129** (2024), 107675. https://doi.org/10.1016/j.cnsns.2023.107675

43. J. Z. Cao, H. Y. Sun, P. M. Hao, P. Wang, Bifurcation and turing instability for a predator-prey model with nonlinear reaction cross-diffusion, *Appl. Math. Modell.*, **89** (2021), 1663—1677. https://doi.org/10.1016/j.apm.2020.08.030

44. X. B. Zhang, Q. An, A. Moussaoui, Effect of density-dependent diffusion on a diffusive predator–prey model in spatially heterogeneous environment, *Math. Comput. Simul.*, **227** (2025), 1–18. https://doi.org/10.1016/j.matcom.2024.07.022

45. W. J. Li, Y. J. Guan, J. D. Cao, F. Xu, A note on global stability of a degenerate diffusion avian influenza model with seasonality and spatial Heterogeneity, *Appl. Math. Lett.*, **148** (2024), 108884. https://doi.org/10.1016/j.aml.2023.108884

46. J. Z. Cao, R. Yuan, Bifurcation analysis in a modified Lesile–Gower model with Holling type II functional response and delay, *Nonlinear Dyn.*, **84** (2016), 1341–1352. https://doi.org/10.1007/s11071-015-2572-5

47. W. J. Li, Y. Zhang, J. C. Ji, L. Huang, Dynamics of a diffusion epidemic SIRI system in heterogeneous environment, *Z. Angew. Math. Phys.*, **74** (2023), 104. https://doi.org/10.1007/s00033-023-02002-z

48. W. J. Li, W. R. Zhao, J. D. Cao, L. Huang, Dynamics of a linear source epidemic system with diffusion and media impact, *Z. Angew. Math. Phys.*, **75** (2024), 144. https://doi.org/10.1007/s00033-024-02271-2

49. L. Perko, *Differential Equations and Dynamical Systems*, Springer Science and Business Media, **7470** (2013).

AIMS Press